Batch reverse osmosis (BRO)-adsorption desalination (AD) hybrid system for multipurpose desalination and minimal liquid discharge

Park, Kiho; Albaik, Ibrahim; Davies, Philip; Al-Dadah, Raya; Mahmoud, Saad Mahmoud; Ismail, Mohamed; Almesfer, Mohammed

DOI:
10.1016/j.desal.2022.115945

Document Version
Publisher's PDF, also known as Version of record

Citation for published version (Harvard):
Park, K, Albaik, I, Davies, P, Al-Dadah, R, Mahmoud, SM, Ismail, M & Almesfer, M 2022, 'Batch reverse osmosis (BRO)-adsorption desalination (AD) hybrid system for multipurpose desalination and minimal liquid discharge', *Desalination*, vol. 539, 115945. https://doi.org/10.1016/j.desal.2022.115945

Desalination 539 (2022) 115945

Contents lists available at ScienceDirect

Desalination

journal homepage: www.elsevier.com/locate/desal

Batch reverse osmosis (BRO)-adsorption desalination (AD) hybrid system for multipurpose desalination and minimal liquid discharge

Kiho Park [a,1], Ibrahim Albaik [b,1], Philip A. Davies [b,*], Raya Al-Dadah [b], Saad Mahmoud [b], Mohamed A. Ismail [c,d], Mohammed K. Almesfer [c]

[a] School of Chemical Engineering, Chonnam National University, 77 Yongbong-ro, Buk-gu, Gwangju 61186, Republic of Korea
[b] School of Engineering, University of Birmingham, Edgbaston, Birmingham B15 2TT, UK
[c] Department of Chemical Engineering, College of Engineering, King Khalid University, Abha 61411, Saudi Arabia
[d] Institute of Engineering Research and Materials Technology, National Center for Research, Khartoum 2424, Sudan

HIGHLIGHTS

- A new hybrid BRO-AD system is proposed.
- Low energy consumption and high recovery are the main advantages of the BRO-AD.
- The BRO-AD has wide applicability to brackish water and seawater desalination.
- Simultaneous cooling power and water productions can be achieved by the BRO-AD.
- Minimal or zero liquid discharge can be achieved.

GRAPHICAL ABSTRACT

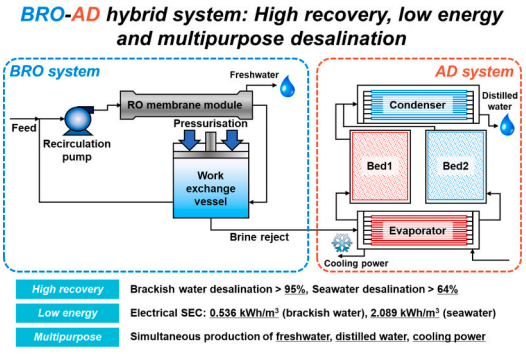

ARTICLE INFO

Keywords:
Batch reverse osmosis
Process modelling
Desalination
Hybrid process
Adsorption desalination
Minimal liquid discharge

ABSTRACT

Brine disposal and energy consumption are the two most important challenges for desalination. In this study, a new hybrid desalination process integrating batch reverse osmosis (BRO) and adsorption desalination (AD) is proposed for high recovery and energy efficiency. Hybrid BRO-AD produces distilled water and drinking water simultaneously. It also provides cooling. Simulation results reveal high recovery of 96.0 % and 64.8 %, low specific electrical energy consumption of 0.536 and 2.089 kWh/m^3, specific thermal energy consumption of 182.3 and 312.2 kWh/m^3, with cooling power generation of 302.5 and 139.5 kW achieved in brackish water and seawater desalination, respectively. The thermal energy consumption can be supplied by low-grade waste heat. The effects of feed concentrations in the ranges of 1–8 g/L (for brackish water) and 30–44 g/L (for seawater) and feed temperature of 25–35 °C are also investigated. The performance of the BRO-AD is compared against non-hybrid BRO and AD systems. The study shows that the BRO-AD hybrid achieves higher recovery than BRO, while reducing the large amounts of adsorbent material needed by AD. With its versatile characteristics, the BRO-AD hybrid system can be considered a breakthrough step in minimal/zero liquid discharge.

* Corresponding author.
E-mail address: p.a.davies@bham.ac.uk (P.A. Davies).
[1] These authors equally contributed to this work.

https://doi.org/10.1016/j.desal.2022.115945
Received 15 March 2022; Received in revised form 24 June 2022; Accepted 27 June 2022
Available online 13 July 2022

Nomenclature

Symbol	Definition
A	Adsorption potential
A_m	Membrane area
A_s	Surface area
A_w	Water permeability
B	Salt permeability
C	Concentration
Cp	Specific heat
D	Diffusivity
d_h	Hydraulic diameter
d_{pipe}	Pipe diameter
Ea	Activation energy of the adsorbent
f	Friction factor
g	Gravitational acceleration
h	Differential head
h_i	Internal heat transfer coefficient
h_{fg}	Heat of evaporation
H	Membrane channel height
J_w	Water flux
K	Mass transfer coefficient
K_o	Pre-exponential constant
k	Thermal conductivity
L	Membrane module length
l	Pipe length
m_{ads}	Adsorbent mass
$\dot{m}$	Mass flow rate
Nu	Nusselt number
P	Pressure
$\overline{P}$	Average pressure
$\widehat{P}$	Peak pressure
PW	Power
Pr	Prandtl number
Q_{st}	Isosteric heat of adsorption
Q_{cond}	Extracted energy from condenser
Q_{evap}	Added energy to evaporator
R	Gas constant
Re	Reynolds number
r	Recovery
S	Mass fraction of salt
S_L	Longitudinal concentration gradient factor
S_P	Concentration polarisation factor
S_R	Salt retention factor
Sc	Schmidt number
Sh	Sherwood number
SEC	Specific energy consumption
T	Temperature
t	Time
V	Volume
$\dot{V}$	Volumetric flowrate
v	Velocity
X_{inf}	Equilibrium water uptake
X	Instantaneous water uptake

Subscripts

ads	Adsorption
aux	Auxiliary units
AD	Adoption desalination system
b	Brine
bk	Bulk
bed	Adsorber bed
BRO	Batch reverse osmose
cond	Condenser
ch	Chilled water
cw	Cold water
des	Desorption
evap	Evaporator
elec	Electrical
hw	Hot water
HX	Heat exchanger
i	Internal
in	Inlet
o	Outer
out	Outlet
p	Pressurisation phase
pipe,R	Retained region in the BRO system
pg	Purged region in the BRO system
r	Purge-and-refill phase
S	Surface
w	Water

Greek letters

ε	surface roughness
ε_t	Total porosity of the adsorbent material
ρ	Density
η	Efficiency
μ	Viscosity
λ	Correction factor
ξ	Minor loss coefficient

1. Introduction

Freshwater is vital to sustain human life. The demand for freshwater is growing rapidly as the human population increases. However, most water on Earth contains salts and cannot be used directly [1]. Therefore, desalination is essential to secure sufficient freshwater for household, agricultural and industrial uses [1]. Various desalination technologies have been developed and implemented as full-scale plants [2,3]. In 2020, the installed desalination capacity 2020 reached over 97.2 million m^3/day [4]. Nonetheless, the large number of desalination plants installed worldwide causes serious problems, especially 1) high energy consumption and CO_2 emissions [2,3] and 2) environmentally harmful effects of brine disposal [5,6]. In 2018, desalination consumed over 75.2 TWh of energy and produced an estimated 52 billion m^3 of brine globally [7,8]. Therefore, there is a need to develop new solutions to alleviate these problems.

Regarding the problems of energy consumption and CO_2 emissions, numerous researchers have investigated new processes and systems to reduce the current level of energy consumption [3,9–14]. Batch reverse osmosis (BRO) has recently been developed to minimise thermodynamically irreversible energy losses in the RO desalination process [15–18]. Because the applied pressure in BRO increases gradually with concentration in the BRO system, the irreversible energy loss is significantly reduced [3,15,19,20]. As a result, the energy consumption of BRO is lower than that of conventional continuous RO, especially at high recovery [14–16,21].

There has been a growing interest and several technological developments in BRO in recent years. These developments have included new configurations to enhance the output and simplify the design of the BRO system [17,22]. Improved models have been developed to represent more accurately the output of BRO including the effects of salt retention and osmotic backflow [23,24]. Experimental and modelling studies have indicated that BRO is likely to resist fouling better than conventional continuous RO [25]. Pilot studies have been carried out

Table 1
AD systems using conventional adsorbent material (silica gel) and newer adsorbent material (MOF), showing improved SDWP using MOF.

References	Adsorbent material	Adsorbent mass (kg)	Study type	Feed salinity (ppm)	SDWP (L/kg/day)	Conclusions
[33]	Silica gel	29.17	Experimental	Up to 30,710	4.69	Met the quality standard for drinking water in China
[29]		36	Numerical and experimental	Up to 86,800	6.7	High purity of water production (15 ppm) with high water recovery (75 %)
[32]		47	Numerical	Up to 220,000	6.5	A slight impact on the SDWP
[34]	Aluminium fumarate (MOF)	23.2	Experimental	Up to 100,000	8.5	Only a reduction of 16.3 % when water salinity increased from 10 to 100,000 ppm. Higher SDWP compared to conventional material using low desorption water temperature
[35]		0.375	Experimental	–	Up to 12	High SDWP but without cooling production – no testing with saline water
[36]	CPO-27 Ni (MOF)	0.67	Numerical and experimental	–	Up to 5 and 15 at desorption water temperature of 95 °C and 155 °C respectively	The system is only effective at a high desorption water temperature – no testing with saline water

with a BRO system using a 8-inch spiral wound module, which is representative of large-scale industrial desalination systems [14,15,24,26]. However, the applications so far are at laboratory and precommercial pilot scale (with maximum output of about 20 m^3/day). Therefore, the technological readiness level of BRO can be described as TRL5.

Despite such progress, BRO and RO systems cannot easily increase recovery to a very high value as needed for minimal brine disposal, because the maximum working pressure of RO membrane is limited [27,28]. Although BRO is an attractive solution for energy minimisation, there is still the environmental issue of brine disposal. Therefore, there is a need to investigate other methods for treating brine to ease this disposal problem,

An interesting technology for brine treatment is adsorption desalination (AD). This technology has recently been developed to treat high-salinity brine using low-grade thermal energy [29,30]. The AD system consists of an evaporator, adsorption/desorption beds, and a condenser [31,32]. It can generate a cooling effect in the evaporator, and provide high-quality freshwater (containing <10 ppm of dissolved solids) in the condenser [31]. Therefore, AD can be effectively utilised for dual purposes of desalination and cooling. Several studies investigated AD in terms of the specific daily water production per mass of adsorbent (SDWP), the effect of feed salinity, and the product water quality. Table 1 compares some studies using conventional adsorbent material (i.e. silica gel) and new adsorbent material (i.e. metal organic framework, MOF). The table confirms the trend towards higher SDWP and the ability to handle feed salinities as high as 220,000 ppm (over 6 times the concentration of seawater). Nevertheless, as a thermal desalination process, AD consumes much more energy than membrane processes such as BRO.

Since, unlike RO, the performance of the AD system is not heavily influenced by feed concentration [32], AD can be employed for brine management when integrated with conventional desalination systems such as RO, multi-effect distillation, and humidification-dehumidification [29,31,32,37–39]. The use of AD to treat brine downstream of conventional desalination can further increase the overall recovery in the desalination system and minimise the volume of brine for disposal. In addition, AD enables a multipurpose desalination system that can simultaneously produce freshwater, high-quality distilled water, and cooling power. Thus, hybridisation with AD is an attractive solution, not only to address the environmental problem of brine disposal, but also to provide valuable products (distilled water and cooling) while capturing low-grade thermal energy.

In other words, a hybrid BRO-AD system could be a competitive solution to address the critical issues of energy minimisation and brine management. To the best of the authors' knowledge, the BRO-AD hybrid has not been proposed before. However, this solution requires certain challenges to be overcome. Firstly, BRO is an intermittent system which periodically discharges concentrated brine [15]. Because AD works continuously, hybridisation requires an appropriate configuration and operating strategy to connect these two systems effectively. Hybrid AD systems reported in the literature use desalination technologies other than BRO. Moreover, they use conventional adsorbent materials such as silica gel and zeolite, which have low water uptake due to the limited surface area in the pores [40,41]. As an alternative adsorbent material, MOFs can provide much higher water uptake due to their high surface area, which enhances the performance of the AD [34] and ultimately can improve the overall performance, water recovery, and electrical consumption of the BRO-AD system.

In this study, we propose a new BRO-AD hybrid configuration for multipurpose desalination with minimal liquid discharge, using MOF (aluminium fumarate). Mathematical modelling is developed to estimate the performance of the BRO-AD hybrid system such as energy consumption, water production rate, permeate water quality, and cooling power generation. The applicability of the BRO-AD hybrid system for brackish water and seawater desalination is analysed. The effects of feed conditions, such as concentration and temperature, are investigated comprehensively to identify the appropriate operating conditions of the BRO-AD hybrid system. To reveal the competitiveness of the BRO-AD hybrid system, non-hybrid BRO and AD systems are compared in terms of energy consumption, permeate water quality, and cooling power generation. Finally, the potential for zero liquid discharge (ZLD) or minimal liquid discharge (MLD) is discussed.

As noted above, both BRO and AD are at pilot system level of development (TRL5). As such, commercial units are not yet widely manufactured, and costings for comparison with more established desalination and cooling technologies are not yet available. For this reason, the economic analysis of the BRO-AD is beyond the scope of this study.

2. Process and methods

2.1. Description of BRO-AD hybrid system

In the proposed hybrid system, BRO and AD units are connected sequentially as shown in Fig. 1. It is assumed that, to avoid fouling or scaling in the BRO-AD system, feed water is supplied via an appropriate pre-treatment system according to the composition of the feed water. The BRO unit operates following the established principle of BRO. In the pressurisation phase, the feed water is fed into the left side of a work exchange vessel at a constant flow rate while increasing its pressure by a feed pump. The pressure of the feed water is transferred via a free piston to the water in the right side of the work exchange vessel. During

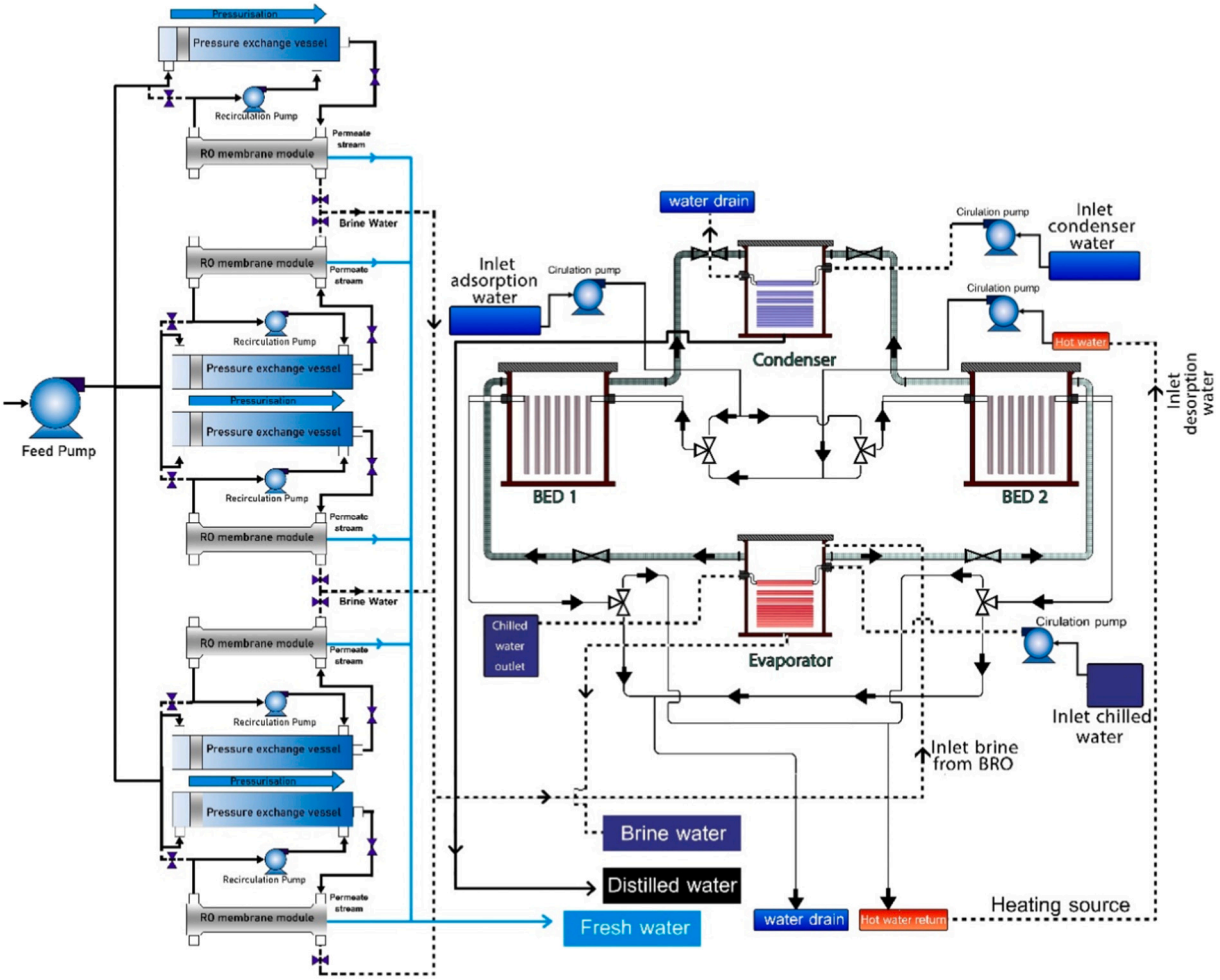

Fig. 1. Schematic illustrations of BRO-AD hybrid process. BRO units are installed for brackish water desalination. The number of BRO units can be adjusted depending on the BRO recovery.

pressurisation, the feed water in the right side of the work exchange vessel flows to a RO module, where permeate water is produced. At the outlet of the RO module, concentrated brine is recirculated by a pump and returns to the work exchange vessel. Because this is a batch operation, the concentration in the BRO unit increases continuously, and the applied pressure of the feed pump should be increased to maintain the constant permeate water production. When the free piston reaches the end of the work exchange vessel, the pressurisation phase finishes, and the purge-and-refill phase begins. In the purge-and-refill phase, the concentrated brine in the BRO unit is discharged, and new feed water is supplied by the feed pump to the BRO unit. At that time, the feed water in the left side of the work exchange vessel is transferred by the recirculation pump to the right side, ready for the start of the next cycle. When the concentration of the discharged brine drops below a certain level, the purge-and-refill phase finishes, and the next pressurisation phase is started.

Downstream of the BRO, the AD cooling and desalination system uses two beds to ensure continuous water and cooling production compatible with the continuous brine discharge from the BRO. During the first half cycle of operation, the first bed operates in adsorption mode by opening the valve between the evaporator and the first bed, while feeding cold water to cool the adsorbent material. The brine in the evaporator starts to evaporate at a specific saturation temperature ($<15\,^{\circ}C$) while the adsorbent material adsorbs the evaporated water, and a cooling effect is generated in the evaporator. Meanwhile, the second bed operates in desorption mode by opening the valve between the condenser and the second bed to allow the stored water in the adsorbent material to be desorbed and condensed in the condenser by feeding hot water to heat up the adsorbent material. A switching time of 40 s is required to switch the processes (adsorption and desorption processes) between the beds. During the switching time, more brine will be accumulated in the evaporator until the adsorption process starts. The required adsorbent mass is determined based on the water recovery of the AD.

The strategy for continuous operation is as follows. Multiple BRO units are connected in parallel, such that pressurisation and purge phases are staggered to provide continuous flow of brine to the AD (see Fig. 2). In the AD, the two adsorption beds operate alternately to handle this continuous brine input.

2.2. Mathematical modelling

To simulate the BRO-AD hybrid process, mathematical models for BRO and AD were used. The BRO and AD models have been validated individually in previous studies [15,34,35,42,43]. The BRO model was developed and validated by designing the same size of work exchange vessel and RO module for pilot-scale water production [15]. The AD model is validated with the SDWP value obtained from experimental work using a packed rectangular finned tube with aluminium fumarate [34]. The experimental SDWP value was 8.5 L/kg/day, while the SDWP for the current study is 8.67 L/kg/day using a chilled water temperature of $24\,^{\circ}C$, desorption temperature of $85\,^{\circ}C$, adsorption and condenser

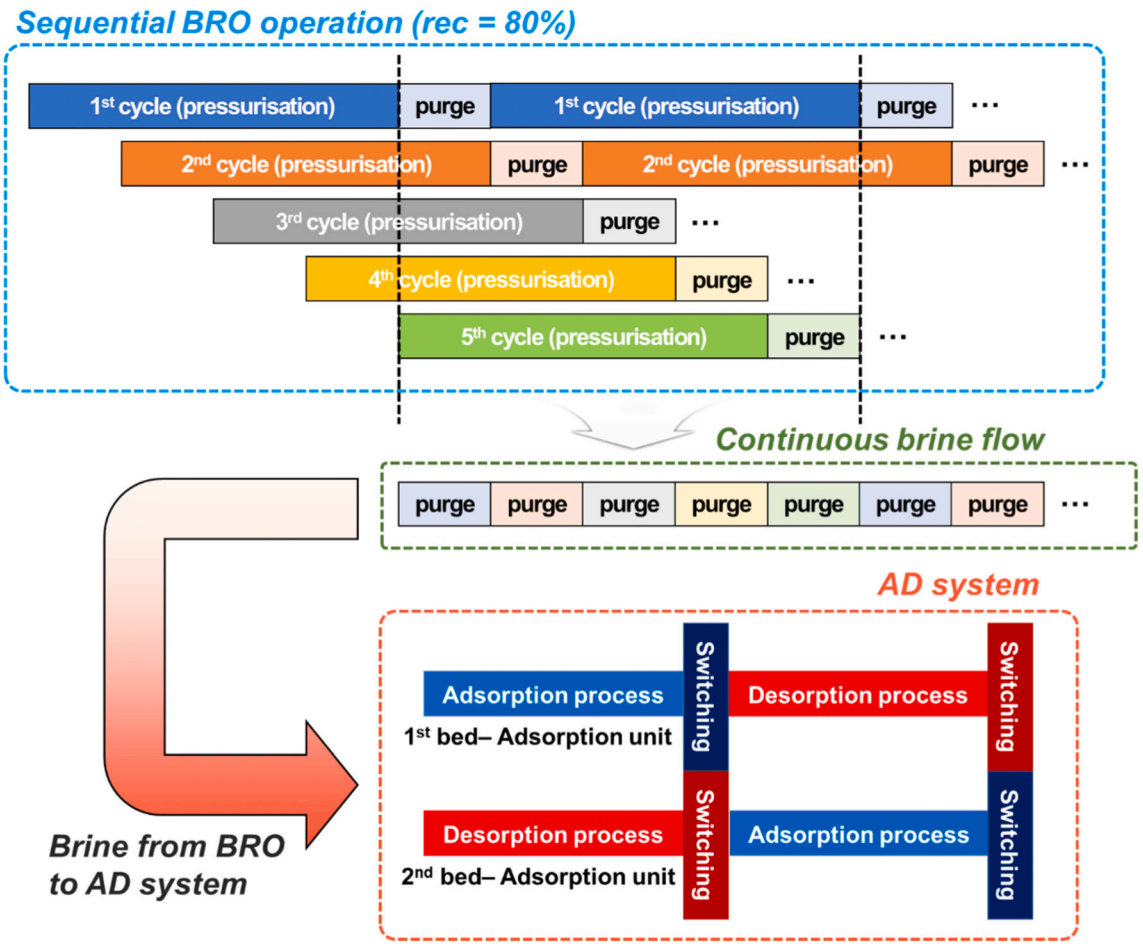

Fig. 2. Operating strategy for continuous water production in BRO-AD hybrid system, showing arrangement of five BRO units operated in staggered sequence for brackish water (3 g/L) desalination at 80 % recovery at the BRO stage, giving 95 % overall recovery. For seawater desalination (35 g/L), with two BRO units operating alternately, BRO recovery is lowered to 50 %, giving 66 % overall recovery.

water temperature of 25 °C, thus showing good agreement with the experimental work with a deviation of only 2 %. The results from the BRO model were used as input conditions for the downstream AD model (see Fig. 2). A simulation program was developed using MATLAB R2020b.

2.2.1. BRO system

The modelling covers the alternating pressurisation and purge-and-refill phases of BRO [21]. In this study, it is assumed that BRO is implemented using a configuration with a free piston developed by Davies et al. [15,21]. The configuration is designed by arranging commercial units such as a pressure exchange vessel, a RO module, and pumps appropriately as described in the previous papers. The alternative arrangement using the flexible bladder by Lienhard et al. [24,44] could be expected to give generally similar results to the free piston. Mathematical modelling equations for a pilot-scale BRO system with an 8-in. spiral-wound RO module were developed in the previous paper [15] and are utilised in this study.

2.2.1.1. Pressurisation phase. Two pumps (feed pump and recirculation pump) are used in the BRO system. To estimate the energy consumed by each pump, the applied pressure required for BRO operation should be calculated. The concentration of feed solution is increased during the pressurisation phase, as permeate water continuously leaves the batch RO system via the RO membrane module. Thus, the applied pressure should be increased during the pressurisation phase. With an assumption that the salt permeation through the RO membrane is negligible, the average applied pressure in the feed pump during the pressurisation phase can be derived using three nonideal factors as follows [15]:

$$\overline{P}_{p,feed} = S_p S_L S_R \pi_{feed} \frac{1}{r_p} ln \frac{1}{1-r_p} + \frac{J_w}{A_w} + \frac{\Delta P_m}{2} \tag{1}$$

$$\Delta P_m = \frac{f_m \mu v L}{(0.5H)^2} \tag{2}$$

$$v = \frac{\dot{V}_{recir} + 0.5\dot{V}_{feed}}{0.5Hw} \tag{3}$$

$$\pi_{feed} = iC_{feed}RT \tag{4}$$

where, S_P is the concentration polarisation factor, S_L is the longitudinal concentration gradient factor, S_R is the salt retention factor, π_{feed} is the osmotic pressure of the feed solution, r_p is the recovery at pressurisation phase, A_w is the water permeability of the RO membrane, ΔP_m is the pressure drop in the RO membrane module, f_m is the friction factor inside the RO module, L is the RO module length, v is the linear velocity inside the RO module, μ is the solution viscosity, H is the membrane channel height, w is the membrane width, V_{recir} is the recirculation flow rate at the exit of the RO module, V_{feed} is the feed flow rate, i is the ionisation number, C_{feed} is the feed concentration, R is the gas constant, and T is the temperature.

The S_p is obtained from boundary layer film theory as follows [15,45,46]:

$$S_p = \frac{\pi_m}{\pi_{bk}} = exp\left(\frac{J_w}{K}\right) \tag{5}$$

where, π_m and π_{bk} are the osmotic pressure at the surface of the membrane and of the bulk solution, respectively, and K is the mass transfer coefficient. The mass transfer coefficient is usually obtained from Sherwood number analogy.

$$K = \frac{Sh \cdot D}{0.5H} \tag{6}$$

$$Sh = 0.2Re^{0.57}Sc^{0.4} \tag{7}$$

$$Re = \frac{\rho v(0.5H)}{\mu} \tag{8}$$

$$Sc = \frac{\mu}{\rho D} \tag{9}$$

where, D is the diffusivity in the solution, ρ is the density. The values of viscosity, density, and diffusivity are obtained from concentration and temperature of the solution [15].

S_L is a function of recirculation flow ratio (α), which is defined as V_{recir}/V_{feed}. The correlation was derived empirically as follows [15]:

$$S_L = 1 + G\alpha^{-n} \tag{10}$$

where, G and n are the empirical parameters. These parameters can be determined by the recovery of BRO unit, and the information can be found in the previous paper [15].

S_R was obtained from the mass balance equations as follows [15,43]:

$$S_R = \frac{C_0}{C_{feed}} = \left[\frac{1 + \frac{V_{pipe,R}}{V_{pg}}}{1 + (1-r)\frac{V_{pipe,R}}{V_{pg}}}\right]\left[1 + \frac{r\lambda}{1-\lambda}\right] \tag{11}$$

where C_0 is the initial concentration in the batch RO cycle, $V_{pipe,R}$ is the pipe volume in retained region, V_{pg} is the summation of the volume inside the RO membrane element(s), the volume in connecting pipe, and the volume associated with the ports of the membrane-containing vessel, r is the recovery of the BRO unit, and λ is the longitudinal dispersion factor. Detailed information about $V_{pipe,R}$ and V_{pg} can be found in the previous paper [15]. As discussed in the previous studies [15,43], $\lambda = 0.08$ is used in this simulation. Please note that r and r_p are slightly different due to the effect of $V_{pipe,R}$ [15].

The peak pressure at the end of the pressurisation phase is calculated by the following equation [15].

$$\widehat{P}_{p,feed} = S_p S_R \pi_{feed}\frac{1}{1-r_p} + \frac{J_w}{A_w} + \frac{\Delta P_m}{2} \tag{12}$$

In addition, the applied pressure in the recirculation pump during the pressurisation phase is calculated from the pressure drops in the RO module and pipes, as follows [15]:

$$P_{p,recir} = \Delta P_m + \frac{\rho}{2}\left(f_{pipe}\frac{L_{pipe,in}v_{pipe,in}^2 + L_{pipe,out}v_{pipe,out}^2}{d_{pipe}} + \sum f_i v_i^2\right) \tag{13}$$

where, f_{pipe} is the friction factor in the pipe, L_{pipe} is the lengths of the pipes, d_{pipe} is the inner diameter of the pipes, subscripts $_{in}$ and $_{out}$ are the inlet and the outlet pipe sections before and after the RO module, f_i is the loss coefficient in the i'th fitting or valve; v_{pipe} and v_i are the fluid velocities in the respective pipe sections and fittings (or valve). Darby 3-K method was used to calculate f_i [47]. High recirculation flow rate increases the energy consumption in the recirculation pump, while it reduces S_L and energy consumption in the feed pump. Thus, α should be optimised to minimise overall energy consumption in the pressurisation phase.

Table 2
Membrane and operating parameters used in BRO simulation [15,48].

Parameter	Value
Water permeability at 25 °C, A_w (m/s/Pa)	2.31×10^{-11} (XLE-440) 9.17×10^{-12} (LG-BW440R) 3.46×10^{-12} (LG-SW440R)
Salt permeability at 25 °C, B (m/s)	1.26×10^{-7} (XLE-440) 4.11×10^{-8} (LG-BW440R) 1.21×10^{-8} (LG-SW440R)
Active membrane area, A_m (m^2)	40.8
Feed spacer thickness, H (mm)	0.7112
Length, L (m)	1.02
Channel width, w (m)	40
Retained solution volume V_m (m^3)	0.01451
Pipe volume (purged), $V_{pipe,pg}$ (m^3)	0.00037
Pipe volume (retained), $V_{pipe,R}$ (m^3)	0.00133
Port dead volume, V_{ports} (m^3)	0.00126
Purged volume, V_{pg} (m^3)	0.0161
Work exchanger volume, V_{b0} (m^3)	0.0646
Feed pump efficiency, η_{feed} (%)	70
Recirculation pump efficiency, η_{recir} (%)	50
Ionisation number, i (-)	1.8648
Friction factor inside the RO module, f_m (-)	20
Friction factor in the pipe, f_{pipe} (-)	0.03008
Longitudinal dispersion factor, λ (-)	0.08
Feed temperature, T (°C)	25–35
Feed concentration, C_{feed} (g/L)	1–8 (brackish water) 30–44 (seawater)
Feed flow rate, $\dot{V}_{feed}$ (L/h)	3000 (brackish water) 1200 (seawater)
Number of parallel BRO unit (-)	5 (brackish water) 2 (seawater)

The permeate concentration during the pressurisation phase is calculated as follows [15]:

$$C_{perm} = \frac{B \cdot A_m}{\dot{V}_{feed}} S_p S_L S_R C_{feed}\frac{1}{r_p} ln\frac{1}{1-r_p} \tag{14}$$

where B is the salt permeability of the RO membrane and A_m is the membrane area in the RO module(s).

Finally, specific energy consumption (SEC) in the pressurisation phase is calculated as follows:

$$SEC_p = \frac{\overline{P}_{p,feed}}{\eta_{feed}} + \frac{P_{p,recir} \cdot \alpha}{\eta_{recir}} \tag{15}$$

2.2.1.2. Purge-and-refill phase. During the purge-and-refill phase, the applied pressure in the feed and recirculation pumps is simply obtained from the pressure drop in the pipes and RO module. Therefore, the applied pressure in the feed ($P_{r,feed}$) and recirculation pumps ($P_{r,recir}$) can be calculated by the same method in Eq. (13). Then, SEC in the purge-and-refill phase is calculated as follows [15]:

$$SEC_r = \frac{P_{r,feed}V_{pg}}{\eta_{feed}V_{b0}} + \frac{P_{r,recir}}{\eta_{recir}} \tag{16}$$

where, V_{b0} is the work exchanger volume. Finally, the overall electrical SEC (SEC_{elec}) in the BRO unit is calculated by considering the auxiliary energy loads (SEC_{aux}) such as controller and electrical valves in the BRO unit as follows [15].

$$SEC_{elec,BRO} = SEC_p + SEC_r + SEC_{aux} \tag{17}$$

The parameters used in the BRO model are summarised in Table 2.

2.2.2. AD system

To simulate the processes in the AD system, mass, energy, water isotherm and kinetics equations are modelled.

2.2.2.1. Conservation of mass. The evaporator has one inlet (the brine from BRO) and two outlets: the brine discharge from the evaporator and

the evaporated water transferred to the active adsorber bed. During the switching time, the evaporation of water is paused. Therefore, to determine the rate of change of mass in the evaporator $\left(\frac{dm_{evap}}{dt}\right)$, the mass balance equation is used as follows:

$$\frac{dm_{evap}}{dt} = \dot{m}_{BRO,b} - \dot{m}_{AD,b} - \varnothing m_{ads}\frac{dX}{dt} \tag{18}$$

where m_{ads} is the adsorbent material mass, $\dot{m}_{BRO,b}$ is the brine mass flow rate from BRO system, $\dot{m}_{AD,b}$ is the brine mass flow rate of AD system, X is the instantaneous water uptake fraction by the active adsorber bed, and $\varnothing$ equals 1 during the adsorption process and 0 during the switching time.

Similarly, the salt balance equation in the evaporator gives:

$$m_w\frac{dS_{evap}}{dt} = \dot{m}_{BRO,b}.S_{BRO,b} - \dot{m}_{AD,b}.S_{AD,b} - \varnothing.S_{ads}\, m_{ads}\frac{dX}{dt} \tag{19}$$

where S is the mass fraction of salt in each case, as indicated by the respective subscripts.

2.2.2.2. Conservation of energy. Starting with the energy balance equation of the evaporator, based on the inlet and outlet streams of fluid, the energy equation can be written as follows:

$$\begin{aligned}(m_{HX}Cp_{HX} + m_wCp_w)\frac{dT_{evap}}{dt} &= h_f m_{BRO,b} - h_f\dot{m}_{AD,b} \\ &- \varnothing h_{fg}\, m_{ads}\frac{dX}{dt} + \dot{m}_{ch}Cp_{ch}\left(T_{ch,in} - T_{ch,out}\right)\end{aligned} \tag{20}$$

where m_{HX} and Cp_{HX} are respectively the mass and specific heat of the heat exchanger in the evaporator, h_f and h_{fg} are respectively the enthalpy of liquid and the latent heat of evaporation, $\dot{m}_{ch}$ is the chilled water flow rate, Cp_{ch} is the specific heat of the chilled water and $T_{ch,\,in}$ and $T_{ch,\,out}$ are the chilled water inlet and outlet temperatures respectively.

The left-hand side of Eq. (20) represents the rate of change of sensible heat stored in the evaporator (heat exchanger and water content). The right-hand side represents the heat added by the brine water from the BRO, rate of heat removed by the discharged brine from the evaporator, the rate of heat extracted due to the evaporation and the rate of heat extracted from the chilled water that passes through the heat exchanger coils respectively.

In each bed, the energy balance equation is based on the process (adsorption or desorption). Cold water inlet/outlet is used during the adsorption process, while hot water inlet/outlet is used during the desorption process. Therefore, the energy balance is calculated as follows:

$$\begin{aligned}&(m_{HX}Cp_{HX} + m_wCp_w + m_{ads}Cp_{ads})\frac{dT_{bed}}{dt} \\ &= \varnothing Q_{st}\, m_{ads}\frac{dX}{dt} + \mathrm{m}_{cw/hw}Cp_{cw/hw}\left(T_{cw/hw,in} - T_{cw/hw,out}\right)\end{aligned} \tag{21}$$

where Q_{st} is the isosteric heat of adsorption and $\dot{m}_{cw/hw}$ is the mass flow rate of the cold/hot water.

The left side of Eq. (21) represents the rate of required heat to be extracted/added heat from/to the heat exchanger in the bed, adsorbed water inside the pores of the adsorbent material and the solid adsorbent material. While the right side of the equation represents the generated/extracted heat during adsorption/desorption process and the heat transferred to/from the thermal fluid during adsorption/desorption processes.

In the condenser, there is one inlet from the desorber bed and one outlet to discharge the condensed distilled water during the desorption process. The energy balance equation is similarly calculated as follows:

$$\begin{aligned}(m_{HX}Cp_{HX} + m_wCp_w)\frac{dT_{cond}}{dt} &= -h_f\dot{m}_{AD,dis} + \varnothing h_{fg}m_{ads}\frac{dX}{dt} \\ &+ \dot{m}_{cond}Cp_{cond}\left(T_{cond,in} - T_{cond,out}\right)\end{aligned} \tag{22}$$

where $\dot{m}_{AD,distilled}$ is the mass flow rate of the discharge of distilled water from the condenser.

The left side of Eq. (22) represents the rate of the extracted heat from the heat exchanger and distilled water of the condenser respectively, while the right-hand side represents the extracted heat from the outlet distilled water, added heat due to the condensation, and the rate of heat transfer to the cooling water of the condenser.

2.2.2.3. Isotherm and kinetics. Aluminium fumarate (AF) is the adsorbent material chosen. It is a MOF material with several advantages over conventional materials, such as high porosity, higher surface area and tuneable molecular adsorption sites [35]. AF can also be regenerated using relatively low temperature (<90 °C) and maintains a good performance in the AD system. The maximum water uptake of AF is 0.56 (kg_w/kg_{ads}) using particle size of 0.12 mm [35]. The AF isotherm (Dubinin-Astakhov (DA) model) equations which represent the relation between the relative pressure and water uptake were developed by Elsayed et al. as the following equations [42]:

$$X_{inf} = 0.111993\, e^{-0.000258797\mathrm{A}}\ (\mathrm{A} > 3987) \tag{23}$$

$$X_{inf} = 2.36129 - 9.93768(10)^{-4}\mathrm{A} + 1.05709(10)^{-7}\mathrm{A}^2\ (2900 \le \mathrm{A} \le 3987) \tag{24}$$

$$\begin{aligned}X_{inf} &= 0.5948 - 3.12(10)^{-4}\mathrm{A} + 1.68302(10)^{-7}\mathrm{A}^2 \\ &- 3.124455(10)^{-11}\mathrm{A}^3\ (\mathrm{A} < 2900)\end{aligned} \tag{25}$$

where X_{inf} is the equilibrium water uptake and A is the adsorption potential that can be calculated using the following equation:

$$A = -RTln\left(\frac{P}{P_o}\right) \tag{26}$$

where P/P_o is the relative pressure between the saturation pressure in the evaporator/condenser to the saturation pressure at adsorbent material temperature.

The developed linear driving force (LDF) equation by Glueckauf [49] is used to describe the kinetics of the adsorbent material as follows:

$$\frac{\mathrm{dX}}{dt} = K\left(X_{inf} - X\right) \tag{27}$$

$$K = K_o\, exp\left(\frac{-E_a}{RT}\right) \tag{28}$$

where X_{inf} is the equilibrium water uptake, X is the instantaneous water uptake, K is the mass transfer coefficient, K_o is the Pre-exponential constant and E_a is the activation energy. The AF isotherm model, the adsorbent potential of the isotherm model, and activation energy and mass transfer coefficient of the kinetic model were already tested and validated in literature [42,50].

2.2.2.4. Heat transfer. The overall heat transfer coefficients (U) in each heat exchanger of the AD system (evaporator, condenser and adsorber bed) and the surface area of the heat exchanger are used to calculate the outlet water temperature based on the following equation:

$$T_{out} = \frac{UA_s\ \mathrm{LMTD}}{\dot{m}Cp} + T_{in} \tag{29}$$

where A_s is the surface area of the heat exchanger and LMTD is the logarithmic mean temperature between heat exchanger, inlet and outlet thermal fluid temperatures.

Table 3
Input parameters for AD system model [34,50].

Parameter	Value
Adsorbent bulk density, ρ_{bulk} (kg/m^3)	520
Isosteric heat of adsorption, Q_{st} (kJ/kg)	2370
Thermal conductivity of metal tube in condenser/adsorber bed, $k_{t\ (cond/bed)}$ (W/m/K)	385 (copper)
Thermal conductivity of metal tube in evaporator, $k_{t\ (evap)}$ (W/m/K)	15 (stainless steel)
Thermal conductivity of fins in adsorber bed, $k_{f\ (bed)}$ (W/m/K)	205 (Aluminium)
Thermal conductivity of adsorbent material, k_{ads} (W/m/K)	0.12
Specific heat of adsorbent, Cp_{ads} (J/kg/K)	970
Activation Energy, E_a (J/mol)	1.80×10^4
Pre-exponential constant, K_o (1/s)	1.29
Surface roughness, ε (mm)	0.0013
Specific heat of the thermal fluid, $Cp_{(ch,cond,cw,hw)}$ (J/kg/K)	4180
Latent heat of evaporation, h_{fg} (kJ/kg)	2400
Prandtl number of the inlet water to the adsorber bed, Pr_{bed} (-)	5.98
Prandtl number of the chilled water inlet, Pr_{ch}(-)	7.77
Prandtl number of the chilled water inlet, Pr_{ch}(-)	5.48
Hydraulic diameter tube in the evaporator and condenser, $d_{h\ (evap/cond)}$ (mm)	14
Hydraulic diameter tube in the adsorber bed, $d_{h(bed)}$ (mm)	9.54

The overall heat transfer coefficient in the evaporator, condenser, and bed heat exchangers, three thermal resistances occur in series, represented by the following equation:

$$UA_s = \frac{1}{R_i + R_{tube} + R_o} \tag{30}$$

R_{tube} is the metal tube thermal resistance, R_o is the outer thermal resistance and R_i is the internal thermal resistance of the heat exchangers, which depends on the thermal fluid used, and is calculated using the following equations.

$$R_i = \frac{1}{h_i A_s} \tag{31}$$

$$h_i = \frac{\mathrm{Nu\ k}}{D_{tube}} \tag{32}$$

$$\mathrm{Nu} = \frac{\frac{f}{8}(Re - 1000)Pr}{1 + 12.7\sqrt{\frac{f}{8}}\left(Pr^{\frac{2}{3}} - 1\right)} \ when\ 3000 < Re < 5(10)^6\ and\ Nu = 4.36\ when\ Re < 3000 \tag{33}$$

The friction factor f is given by:

$$f = \frac{1}{\left(1.8log_{10}\left(\frac{6.9}{Re} + \left(\frac{\frac{\varepsilon}{d}}{3.7}\right)^{1.11}\right)\right)^2} \tag{34}$$

where h_i is the internal heat transfer coefficient, Nu is the Nusselt number, Pr is the Prandtl number, and ε is the surface roughness.

As the heat exchanger in the beds is a finned-tube type and packed with the granular adsorbent material that has a thermal contact resistance, the outer heat transfer coefficient in the adsorber bed is calculated using the model of Rezk et al. [51]. While the outer heat transfer coefficient in the evaporator is based on the nucleate pool boiling in the flooded evaporator and is based on laminar falling film condensation over horizontal tubes in the condenser.

The input parameters of the AD system are summarised in Table 3.

To combine the AD unit with the BRO, the operating temperatures and cycle time (see Table 4) of the AD unit is adjusted to ensure having distilled water production as well as cooling power at low temperature (<20 °C).

2.2.2.5. AD cycle performance. To indicate the performance of the AD system, SDWP, specific cooling power (SCP) and thermal coefficient of performance (COP) are calculated using the following equations:

Table 4
Operating conditions of AD system.

Parameter	Unit	Value
Inlet brine water temperature from BRO	°C	25, 30 and 35
Inlet adsorption water temperature		
Inlet condenser water temperature		
Inlet chilled water temperature	°C	24
Inlet desorption water temperature	°C	90
Half cycle time	s	300
Switching time	s	40

$$\mathrm{SDWP} = \int_0^{tcycle} \frac{Q_{cond}}{h_{fg} M_{ads}} dt \tag{35}$$

$$\mathrm{SCP} = \int_0^{tcycle} \frac{Q_{evap}}{M_{ads}} dt \tag{36}$$

$$\mathrm{Thermal\ COP} = \int_0^{tcycle} \frac{Q_{evap}}{Q_{des}} dt \tag{37}$$

where Q_{cond}, Q_{evap} and Q_{des} are the energy transferred in the condenser, evaporator, and desorber bed, respectively. Because the thermal energy consumption is significantly higher than the pump energy consumption (by a factor of >100), the pump electrical power was neglected in the COP calculation. Thus, we discuss only thermal COP. It should be noted that the electrical energy consumption was not ignored in the SEC calculation as shown in the next section.

2.2.2.6. Specific electrical and thermal energy consumptions. The electrical energy consumption in the AD system is mainly that of pumping water to the heat exchanger coils in the evaporator and condenser and the packed finned tube in the adsorber bed. The electrical pumping power is calculated using the following equation:

$$PW_{elec} = \eta \frac{q\ \rho\ g\ h}{3.6 \times 10^6} \tag{38}$$

where PW_{elec} is the electrical pumping power (kW), q is the flow rate (m^3/h), g is the acceleration of gravity (m/s^2), and h is the differential head (m).

The differential head consists of the minor loss (h_{minor}) (due to components in the system such as elbows and valves) and major loss (h_{major}) (due to friction in the pipe). The major loss is calculated as follows:

$$h_{major} = \mathrm{f}\frac{l\ v^2}{2g\ d_h} \tag{39}$$

where f is the friction coefficient of the copper pipes in condenser/adsorber bed and stainless pipes in evaporator [52], l is the pipe length, d_h is the hydraulic diameter and v is the fluid velocity (m/s).

For the evaporator and condenser, the required pipe length is calculated based on the required surface area of the pipes (outer diameter of 15 mm), according to the heat transfer coefficients obtained from Eqs. (29)–(34). For the adsorbed bed, the pipe length is calculated based on the required amount of adsorbent material given that each packed heat exchanger modules consists of 8 parallel finned tubes with outer diameter of 9.54 mm, length of 800 mm, fin spacing of 2 mm, and fin height of 8.5 mm. The velocity in all pipes is 0.5 m/s.

The minor head loss is calculated as follows:

$$h_{\mathrm{minor}} = \xi\frac{v^2}{2g} \tag{40}$$

where ξ is the minor loss coefficient (0.05 for ball valve, 7 for flowmeter, 1.5 for 180° elbow and 1 for inlet and outlet) [52].

Thus, the $SEC_{elec,AD}$ is calculated as follows:

$$SEC_{elec,AD} = \frac{24.PW_{elec}}{SDWP.m_{ads}} \quad (41)$$

Regarding the thermal consumption in AD system, which is calculated from the required heating energy during the desorption process, the following equation is used:

$$SEC_{heat,AD} = \left(\frac{SCP.m_{ads}}{\text{thermal COP}}\right).\frac{24}{SDWP.m_{ads}} \quad (42)$$

where $\left(\frac{SCP.m_{ads}}{\text{thermal COP}}\right)$ is the heating power (kW).

The overall electrical and thermal SEC in the BRO-AD hybrid system are expressed as follows:

$$SEC_{elec} = \frac{SEC_{elec,BRO} \bullet \dot{V}_{feed} + SEC_{elec,AD} \bullet \dot{V}_{cond}}{\dot{V}_{feed} + \dot{V}_{cond}} \quad (43)$$

$$SEC_{heat} = \frac{SEC_{heat,AD} \bullet \dot{V}_{cond}}{\dot{V}_{feed} + \dot{V}_{cond}} \quad (44)$$

$\dot{V}_{cond}$ is the distilled volumetric flow from the condenser (m^3/h), which is calculated using the following equation:

$$\dot{V}_{cond} = \frac{SDWP\ m_{ads}}{24000} \quad (45)$$

To study the salinity effect on the water production of the AD, a linear equation is considered based on the experimental study carried out by Albaik et al. [34] for a salinity concentration of up to 100,000 ppm (100 g/L). The results showed that the SDWP decreased by only 16.3 % when the salinity concentration increased from 90 to 100,000 ppm (0.09 to 100 g/L). The reduction percentage on the water production is calculated as follows:

$$SE = (0.001382626\ BC) + 0.010087 \quad (46)$$

where SE is the salinity effect and BC is the brine concentration from the BRO system.

The adsorbent mass is calculated based on feed water salinity and temperature while ensuring that the water salinity of the brine water discharged from the AD system does not exceed 130,000 ppm, such that the heat transfer coefficient in the evaporator is not affected significantly by the water salinity. To apply the SE in the model, the rate of the water uptake $\frac{dX}{dt}$ in the LDF equation (Eq. (27)) is multiplied by (1-SE).

3. Results and discussion

3.1. Baseline case analysis for BRO-AD hybrid system

So that the effect of varying operating parameters can be studied, a baseline is needed. Two baseline cases were defined with respect to the feed to the BRO: brackish water feed (3 g/L concentration) and seawater feed (35 g/L concentration). The BRO recovery is fixed at 80 % (for brackish water) and 50 % (for seawater). Since each BRO unit is designed to treat 600 L/h of feed flow rate, five brackish water or two seawater units were employed, in each case requiring a total feed flow of 3000 L/h and 1200 L/h respectively. The water production rate can be adjusted by increasing the number of BRO units in brackish water and seawater desalination. However, the overall SEC would not change because the SEC of each unit is fixed. Therefore, the calculation is based on the minimum number of BRO units (5 units for brackish water desalination and 2 units for seawater desalination) for continuous production of brine to feed the AD. The sequential operation of BRO units was described in Fig. 2. In both cases, the evaporator saline feedwater temperature was 25 °C, while the operating temperatures of the AD system were 25 °C, 90 °C, 24 °C, and 25 °C corresponding respectively to the temperatures of adsorber bed cooling water inlet, desorber bed heating water inlet, evaporator chilled water inlet, and the condenser cooling water inlet.

Table 5
Simulation results for the baseline case of BRO-AD hybrid system, brackish water desalination, using high-flux RO membrane (XLE-440 from Dupont).

	BRO unit in BRO-AD system	AD unit in BRO-AD system	Overall process (BRO-AD)
SEC_{elec} (kWh/m^3)	0.348	1.476	0.536
SEC_{heat} (kWh/m^3)	N/A	1096	182.3
Peak pressure (kPa)	1563	N/A	1563
Freshwater production rate (L/h)	2400	N/A	2400
Freshwater concentration (g/L)	0.238	N/A	0.238
Distilled water production rate (L/h)	0	478.6	478.6
Distilled water concentration (g/L)	N/A	0.01	0.01
Recovery (%)	80	79.76	95.95
Brine concentration (g/L)	14.05	59.83	59.83
Cooling power (kW)	N/A	302.5	302.5
Thermal COP (-)	N/A	0.58	0.58

Table 6
Simulation results for the baseline case of BRO-AD hybrid system, brackish water desalination, using high-rejection RO membrane (LG-BW440R from LG Chem).

	BRO unit in BRO-AD system	AD unit in BRO-AD system	Overall process (BRO-AD)
SEC_{elec} (kWh/m^3)	0.439	1.481	0.611
SEC_{heat} (kWh/m^3)	N/A	1100	182.4
Peak pressure (kPa)	1790	N/A	1790
Freshwater production rate (L/h)	2400	N/A	2400
Freshwater concentration (g/L)	0.065	N/A	0.065
Distilled water production rate (L/h)	0	476.7	476.7
Distilled water concentration (g/L)	N/A	0.01	0.01
Recovery (%)	80	79.44	95.89
Brine concentration (g/L)	14.74	62.18	62.18
Cooling power (kW)	N/A	301.6	301.6
Thermal COP (-)	N/A	0.575	0.575

3.1.1. Baseline case for brackish water desalination

Tables 5 and 6 show the baseline results for brackish water desalination with the high-flux membrane (XLE-440 from Dupont) and high-rejection membrane (BW440R from LG Chem.), respectively. In both cases, the BRO-AD hybrid system can operate at very high recovery of over 95 %, achieved by initial recovery of 80 % in the BRO, followed by final recovery of >75 % in the downstream AD. With the high-flux membrane, SEC is 0.536 kWh/m^3 (electrical) and 182.3 kWh/m^3 (thermal). The SEC_{elec} is small compared to that reported for conventional brackish water reverse osmosis (BWRO) processes (0.6–1.7 kWh/m^3) which normally operate at recovery of only 70–80 % [53–55]. Thus, SEC_{elec} in BRO-AD hybrid system is low considering the high recovery, confirming suitability for ZLD and MLD applications [27]. Although the BRO-AD hybrid system requires substantial thermal energy, there are many applications where this thermal energy is available from low-grade thermal resources. The heating input of 90 °C can be obtained from industrial waste heat, solar, and geothermal energy [56]. The low-grade thermal energy could alternatively be used for power generation via organic Rankine cycle (ORC) or pressure retarded membrane distillation (PRMD) [57,58]. However, the low conversion efficiency of these processes is a drawback. Therefore, the direct utilisation of low-

Table 7
Simulation results at the base case of BRO-AD hybrid system (seawater desalination): high-rejection RO membrane (LG-SW440R from LG Chem.)

	BRO unit in BRO-AD system	AD unit in BRO-AD system	Overall process (BRO-AD)
SEC_{elec} (kWh/m^3)	2.213	1.850	2.089
SEC_{heat} (kWh/m^3)	N/A	1364	312.2
Peak pressure (kPa)	7151	N/A	7151
Freshwater production rate (L/h)	600	N/A	600
Freshwater concentration (g/L)	0.197	N/A	0.197
Distilled water production rate (L/h)	0	178.1	178.1
Distilled water concentration (g/L)	N/A	0.01	0.01
Recovery (%)	50	29.68	64.84
Brine concentration (g/L)	69.80	108.4	108.4
Cooling power (kW)	N/A	139.5	139.5
Thermal COP (-)	N/A	0.574	0.574

grade thermal energy in the BRO-AD hybrid system may be beneficial to improve the practicality of low-grade thermal energy capture. Moreover, SEC_{heat} in BRO-AD hybrid system is lower than other thermal desalination systems such as membrane distillation [59] (see Section 3.3 for further comparison).

Besides having low energy consumption, the BRO-AD hybrid also has advantages as a multipurpose desalination system. The freshwater produced by BRO unit has an adequate quality for drinking (0.238 g/L in the case of high-flux membrane and 0.065 g/L in the case of high-rejection membrane). The common drinking water regulation formulated by the US environmental protection agency (EPA) specifies <500 ppm (0.5 g/L) [60]. However, many countries specify below 200 ppm (0.2 g/L) for high-quality drinking water [48]. Thus, this system can meet both requirements through appropriate choice of membrane. In addition, the BRO unit produces distilled water at only 0.01 g/L which can be used in special applications such as food and drinks or pharmaceutical industries. Thus, two different types of permeate can be produced by BRO-AD hybrid system. Furthermore, the temperature of chilled water is cooled down across the AD unit due to the water evaporation (from 24 °C to around 14–18 °C). The generated cooling power is 301.6–302.5 kW and thermal COP is 0.575–0.58 (Tables 5 and 6). Thus, the BRO-AD hybrid system is versatile in providing fresh water, distilled water, and cooling – alongside efficient and high recovery (95 %) performance.

Conventional BWRO cannot readily reach such high recovery because of pressure limitations of the RO membrane. At 3 g/L feed concentration, the osmotic pressure of concentrated brine at 95 % recovery would reach 46.5 bar – exceeding the working pressure of most spiral-wound type BWRO membranes (~41 bar) [61]. Because the actual applied pressure must exceed the osmotic pressure, the current BWRO membranes cannot be used at such high recovery. Although seawater reverse osmosis (SWRO) membranes allow higher working pressure (82.7 bar), their inferior permeability increases feed pressure requirements, incurring a penalty in SEC_{elec} and associated costs [61,62]. In contrast, the peak pressure in BRO-AD hybrid system is only 15.6 bar (with high-flux membrane) and 17.9 bar (with high-rejection

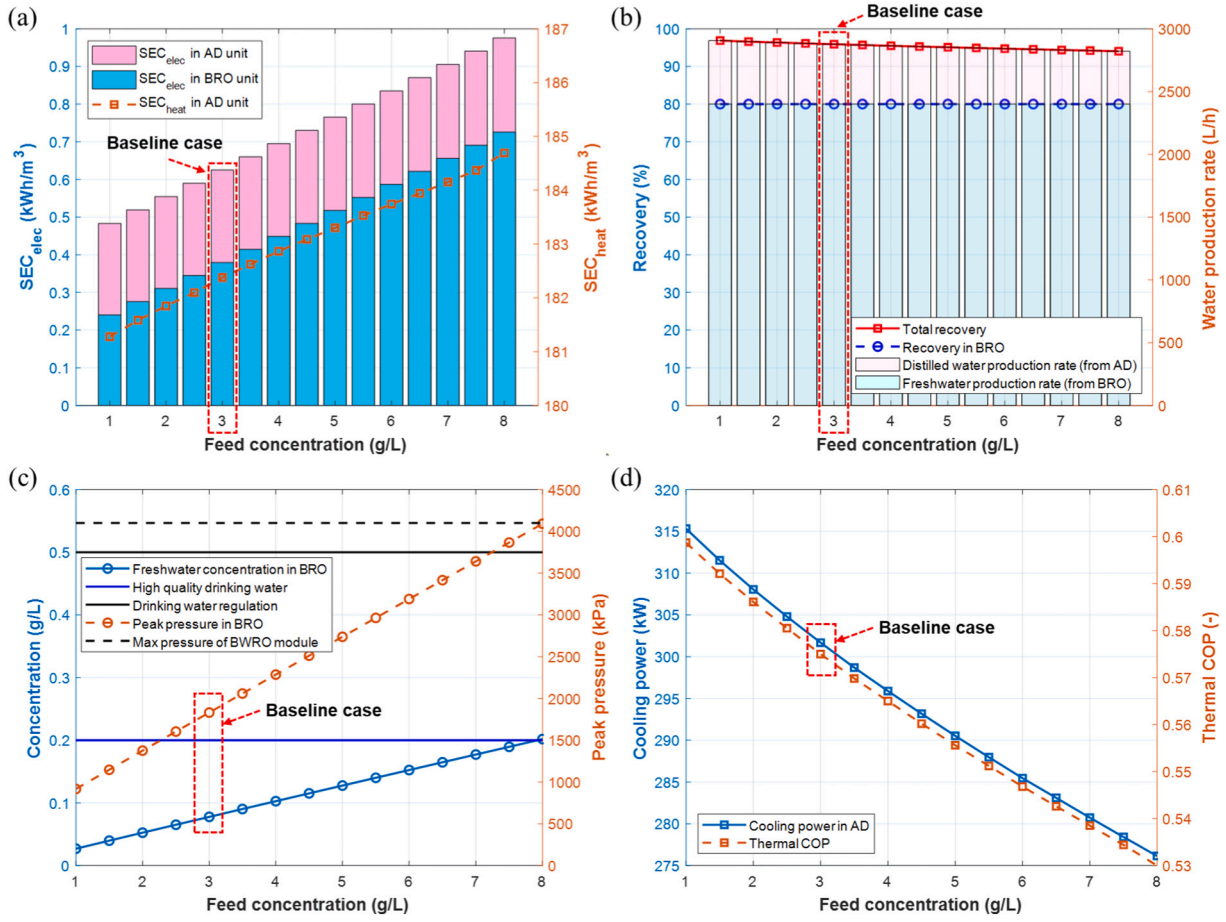

Fig. 3. Effects of feed concentration on the performances of BRO-AD hybrid system for brackish water desalination. High-rejection RO membrane (LG-BW440R from LG Chem). (a) SEC_{elec} and SEC_{heat}, (b) recovery and water production rate in each unit, (c) permeate quality and peak pressure at RO unit, and (d) cooling power and thermal COP.

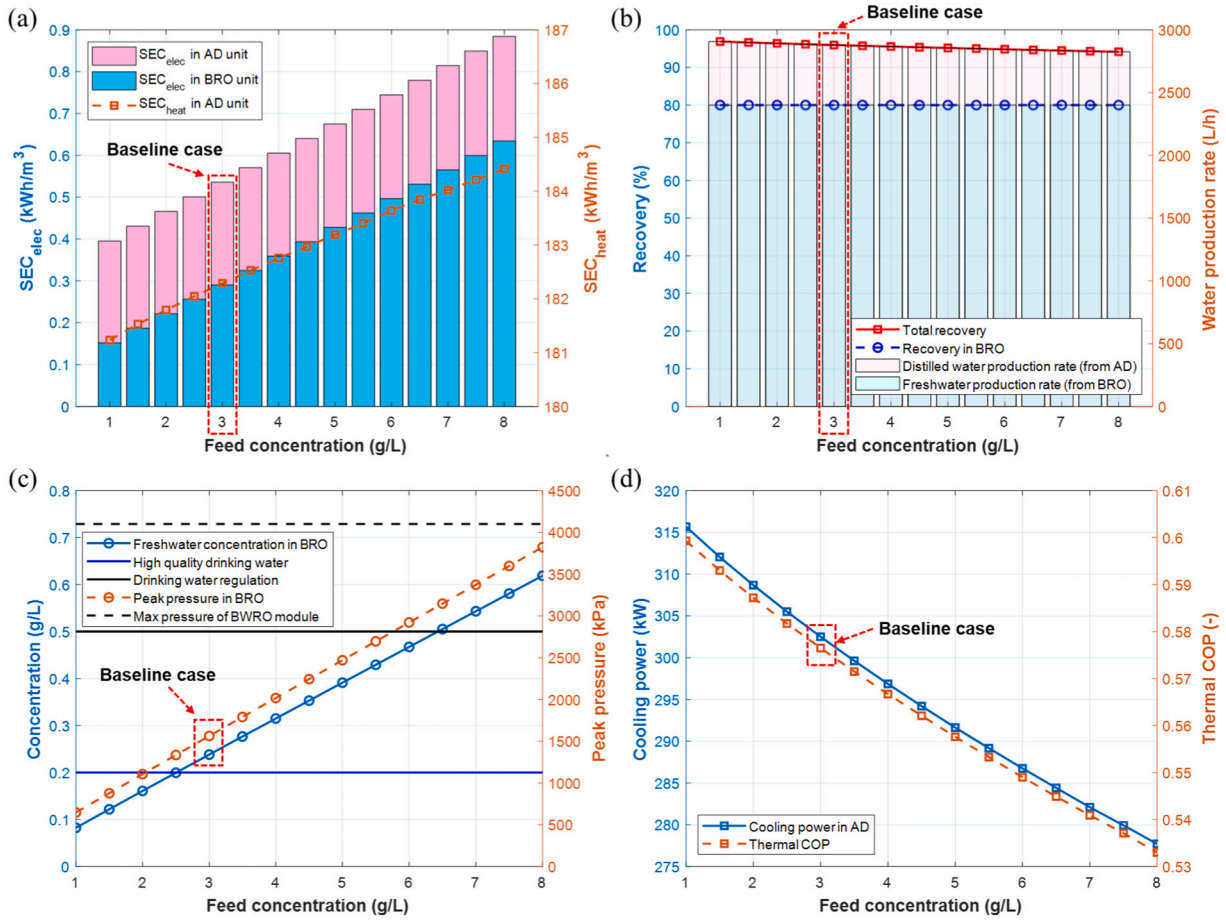

Fig. 4. Effects of feed concentration on the performances of BRO-AD hybrid system for brackish water desalination. High-flux membrane RO membrane (XLE-440 from Dupont). (a) SEC_{elec} and SEC_{heat}, (b) recovery and water production rate in each unit, (c) permeate quality and peak pressure at RO unit, and (d) cooling power and thermal COP.

membrane) even at very high recovery over 95 %.

3.1.2. *Baseline case for seawater desalination*

Unlike in brackish water desalination, only the high-rejection SWRO membrane was studied for seawater desalination, because the permeate concentration using the high-flux SWRO membrane would fail to meet drinking water standards. The recovery of the BRO unit was fixed at 50 %, resulting in an overall recovery 69.8 % for the BRO-AD system. SEC_{elec} and SEC_{heat} in BRO-AD system were 2.098 kWh/m^3 and 312.2 kWh/m^3, respectively (Table 7). By considering that SEC of a single-stage conventional SWRO system at the same feed condition (35 g/L concentration and 25 °C) is around 3.16 kWh/m^3 at 70 % recovery [63], SEC_{elec} of BRO-AD is much lower than that of conventional SWRO. Compared to SEC of both two-stage SWRO (2.6 kWh/m^3) [64] and cascading osmotically mediated RO (COMRO) (2.1–2.2 kWh/m^3) [63], the BRO-AD hybrid has lower SEC_{elec}. In practice, single-stage and two-stage SWRO cannot reach the high recovery (70 %) due to the current pressure limitation [48,64]. Concentration polarisation, pressure losses, and device inefficiencies were not clearly considered in the energy calculation for COMRO [27,65–67], such that the advantage of AD-BRO may in fact be greater than these figures suggest. The peak pressure of BRO-AD hybrid system for seawater desalination is 71.5 bar, well within the upper limit of SWRO membranes. Thus, the BRO-AD hybrid is an efficient option for seawater desalination provided low-grade thermal heat is readily available.

3.2. *Effects of feed salinity and temperature*

The feed salinity and temperature significantly affect the performance of the BRO-AD hybrid system due to the change in feed osmotic pressure. This section studies these effects, in comparison to the two baseline cases (i.e. brackish water and seawater desalination).

3.2.1. *Effect of feed salinity: brackish water case*

Using the high rejection membrane, as the feed salinity increases from 1 g/L to 8 g/L, SEC_{elec} of the BRO-AD system also increases proportionately from 0.483 to 0.976 kWh/m^3 (Fig. 3a). The increase is caused by the increase in osmotic pressure, which affects directly the SEC_{elec} of the BRO unit. Meanwhile, the SEC_{elec} of the AD unit remains almost constant, because electricity is only required to operate transfer pumps and valves, and is thus independent of osmotic pressure. In contrast, the increased brine concentration after the BRO unit decreases the vapour pressure, increasing slightly the SEC_{heat} required by the AD unit. Because the amount of adsorbent is assumed constant, the decreased vapour pressure at higher brine concentration reduces the recovery of the AD unit as shown in Fig. 3b. In this simulation, the recovery in the BRO unit is fixed at 80 % for fair comparison, such that the freshwater production rate of the BRO unit is constant (2400 L/h) over all feed concentrations; whereas the distilled water production rate is decreased as the feed concentration increases. Thus, overall recovery is reduced at higher feed concentration. Nevertheless, overall recovery remains high (>94 %) even up to feed concentration of 8 g/L.

With the high-rejection membrane, the quality of freshwater produced from the BRO unit continues to meet the standard of high-quality

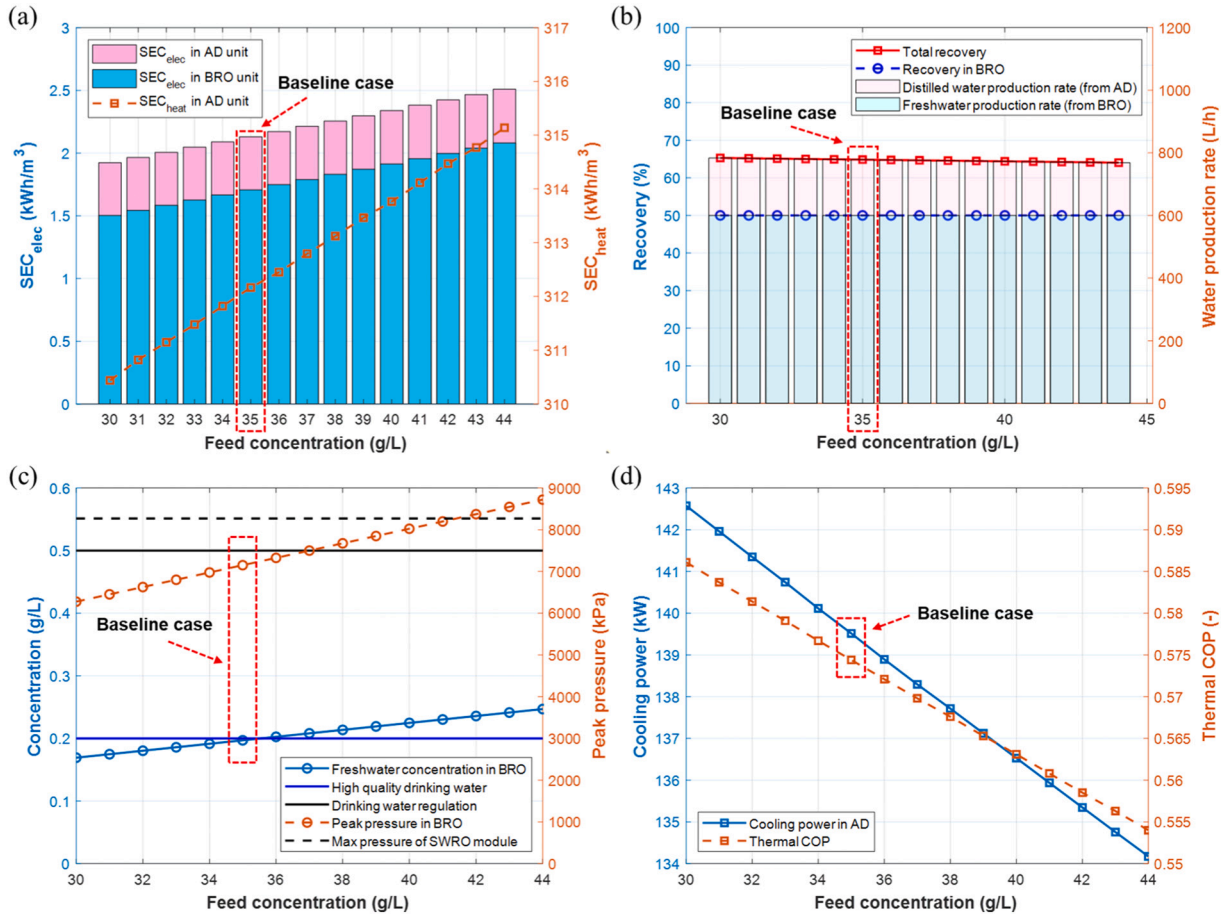

Fig. 5. Effects of feed concentration on the performances of BRO-AD hybrid system for seawater desalination. RO membrane: LG-SW440R (high-rejection membrane) from LG Chem. (a) SEC_{elec} and SEC_{heat}, (b) recovery and water production rate in each unit, (c) permeate quality and peak pressure at RO unit, and (d) cooling power and thermal COP.

drinking water (<0.2 g/L) for all feed concentrations up to 8 g/L (Fig. 3c). Meanwhile peak pressure remains within the 41-bar operating limit of the membrane, and the recovery of BRO-AD hybrid system remains above 94 %. Cooling power generation and thermal COP in the AD unit decrease somewhat, from 315 to 275 W and from 0.6 to 0.53 respectively, because of reduced vapour pressure at higher feed concentration (Fig. 3d). In summary, the results confirm that the unit maintains good performance for a range of brackish water feed concentrations well above the baseline case.

The effect of feed concentration using the high-flux BWRO membrane was also studied (see results in Fig. 4). At the maximum concentration of 8 g/L, the overall SEC_{elec} of the BRO-AD hybrid system with high-flux membrane is 0.884 kWh/m^3 (Fig. 4a). Compared to the high-rejection membrane (0.976 kWh/m^3), the high-flux BWRO membrane is advantageous in providing low-energy consumption, but at the cost of poorer permeate quality. Thus, with feed concentration >2.5 g/L, the freshwater produced by the BRO unit has too high concentration to satisfy the standard of high-quality drinking water. Although it does not necessarily violate the EPA drinking water regulation (0.5 g/L), it might not meet consumer expectations. For example, according to Bruvold and Ongerth, an excellent taste is achieved at <0.3 g/L [68]. Thus, there is a trade-off between energy consumption and water quality.

3.2.2. *Effect of feed salinity: seawater case*

As the concentration of seawater varies with the region and season, the effect of concentration from 30 to 44 g/L was studied. Using the high-rejection membrane, the increase from 30 to 44 g/L increased SEC_{elec} from 1.923 kWh/m^3 to 2.503 kWh/m^3 (see results in Fig. 5a). Regardless of the feed concentration, the proportion of SEC_{elec} consumed in the BRO and AD units is approximately 78 % and 22 %, respectively. The required SEC_{heat} for seawater desalination is around 310.4–315.1 kWh/m^3, much larger than that for brackish water desalination because of lower vapour pressure in the evaporator, as discussed in Section 3.2.1. In terms of SEC_{elec}, the energy consumption in a two-stage SWRO system with internal stage design (ISD) at the 50 g/L feed concentration and 40 % recovery is 3.03 kWh/m^3 [48]. Although the feed concentration of the two-stage SWRO (50 g/L) [48] is higher than the current study (44 g/L), the recovery in this study (64 % as shown in Fig. 5b) is much higher than 40 %. In addition, the pump efficiency in this study (70 %) is lower than the case of two-stage SWRO (80 %) [48]. Considering all factors, SEC_{elec} of BRO-AD hybrid system is much lower than the other configurations like two-stage SWRO. Where low-grade thermal energy is supplied freely or cheaply, the competitiveness of BRO-AD hybrid system will be very significant.

The major barrier to the application of SWRO at high recovery and high salinity seawater desalination is the maximum working pressure of SWRO membranes [27,63,64]. Provided feed concentration is below 42 g/L, the peak pressure in the BRO unit will remain below the maximum pressure limit. In the range 43–44 g/L, the peak pressure slightly exceeds the maximum limit (Fig. 5c). In this range of feed concentration, the BRO-AD hybrid can be operated successfully by lowering the recovery of the BRO unit. Concerning freshwater quality, the freshwater produced by the BRO-AD hybrid system for seawater desalination is in the range of 0.169–0.247 g/L, which can be regarded as high-quality drinking water (Fig. 5c). Cooling power generation, however, falls to around 134.2–142.6 W, which is much lower than in

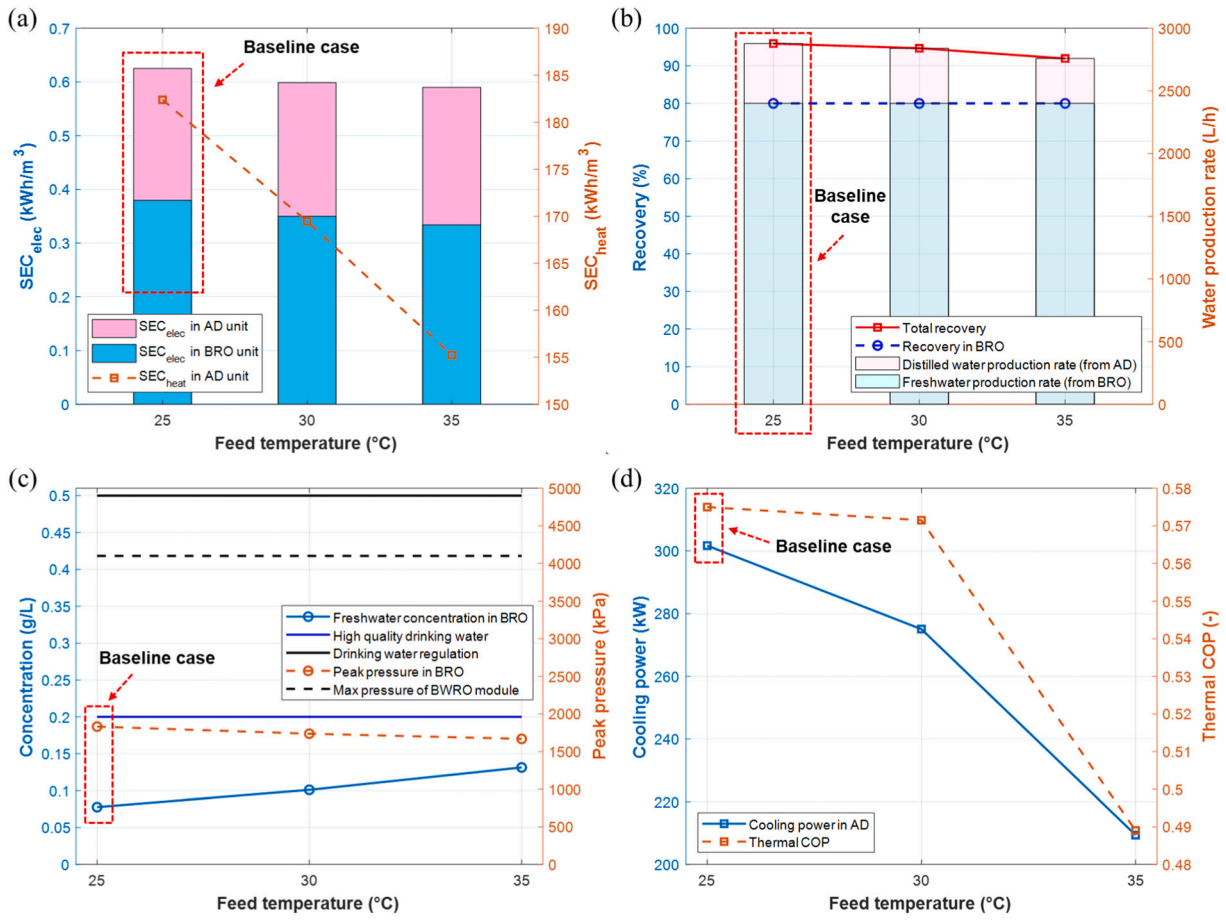

Fig. 6. Effects of feed temperature on the performances of BRO-AD hybrid system for brackish water desalination: high-rejection RO membrane (LG-BW440R) (a) SEC_{elec} and SEC_{heat}, (b) recovery and water production rate in each unit, (c) permeate quality and peak pressure at RO unit, and (d) cooling power and thermal COP.

brackish water desalination (Fig. 5d). As mentioned in Section 3.1, this is because the reduced vapour pressure reduces cooling power and thermal COP.

To investigate the effects of feed temperature, the temperature range was varied from 25 to 35 °C. The higher the feed temperature, the higher the osmotic pressure, which tends to increase the SEC. Meanwhile, the higher feed temperature increases water permeability of the RO membrane, tending to reduce SEC thus leading to a trade-off [48,69]. In addition, the effect of elevated feed temperature on the AD unit are shown in Figs. 6 (brackish water desalination) and 7 (seawater desalination). The temperature correction factor for membrane permeability was taken from reference [48].

3.2.3. *Effect of feed temperature: brackish water case*

As the feed temperature increases, SEC_{elec} in the BRO unit decreases in brackish water desalination (Fig. 6a). Although the osmotic pressure of the feed solution rises with temperature, increased water permeability more than offsets that rise, giving a net reduction in SEC_{elec} of the BRO unit. Regarding the AD unit, SEC_{elec} is increased and SEC_{heat} is reduced at high feed temperature. Because higher temperature of the feed solution reduces the maximum loading in the AD unit, the recovery in the AD unit decreases from 95.89 % (at 25 °C) to 91.94 % (at 35 °C) as shown in Fig. 6b. The reduced recovery increases SEC_{elec} in the AD unit, because the denominator in SEC_{elec} is decreased. The reduced maximum loading in the AD unit decreases SEC_{heat} from 182.4 kWh/m^3 (at 25 °C) to 152.3 kWh/m^3 (at 25 °C). The increased SEC_{elec} in the AD unit is much lower than the reduced SEC_{elec} in the BRO unit. Overall, SEC_{elec} and SEC_{heat} in the BRO-AD hybrid system decrease with increasing feed temperature; however, the overall recovery deteriorates at higher feed temperature.

In addition, the high temperature of the feed solution lowers the permeate water quality and cooling power generation as shown in Fig. 6c and d. The permeate water concentration is increased from 0.078 g/L to 0.131 g/L, and the cooling power is reduced from 301.7 W to 209.4 W, when the feed temperature increases from 25 °C to 35 °C. The peak pressure of the BRO unit is slightly reduced from 18.31 bar (at 25 °C) to 16.52 bar (at 35 °C) by the increased membrane permeability. Thus, although the high temperature operation has lower energy consumption, the decreased quality of permeate water, recovery, and cooling power generation may favour feed water temperature below 25 °C.

3.2.4. *Effect of feed temperature: seawater case*

A similar study was conducted for seawater desalination. The results in Fig. 7 exhibit trends that are mostly similar to the case of brackish water desalination. The only difference is in SEC_{elec} which, unlike in brackish water desalination, increases slightly from 2.13 kWh/m^3 to 2.17 kWh/m^3 as the feed temperature increases from 25 to 35 °C (Fig. 7a). The main reason is the difference in the fraction of desalinated water coming from the BRO and AD units. Compared to brackish water desalination, the relative amount of water produced by the AD unit is much larger. Distilled water from the AD makes up 16.5 % of the total output in brackish water desalination, increasing to 22.8 % in seawater desalination. Thus, the increased SEC_{elec} in the AD unit has a larger

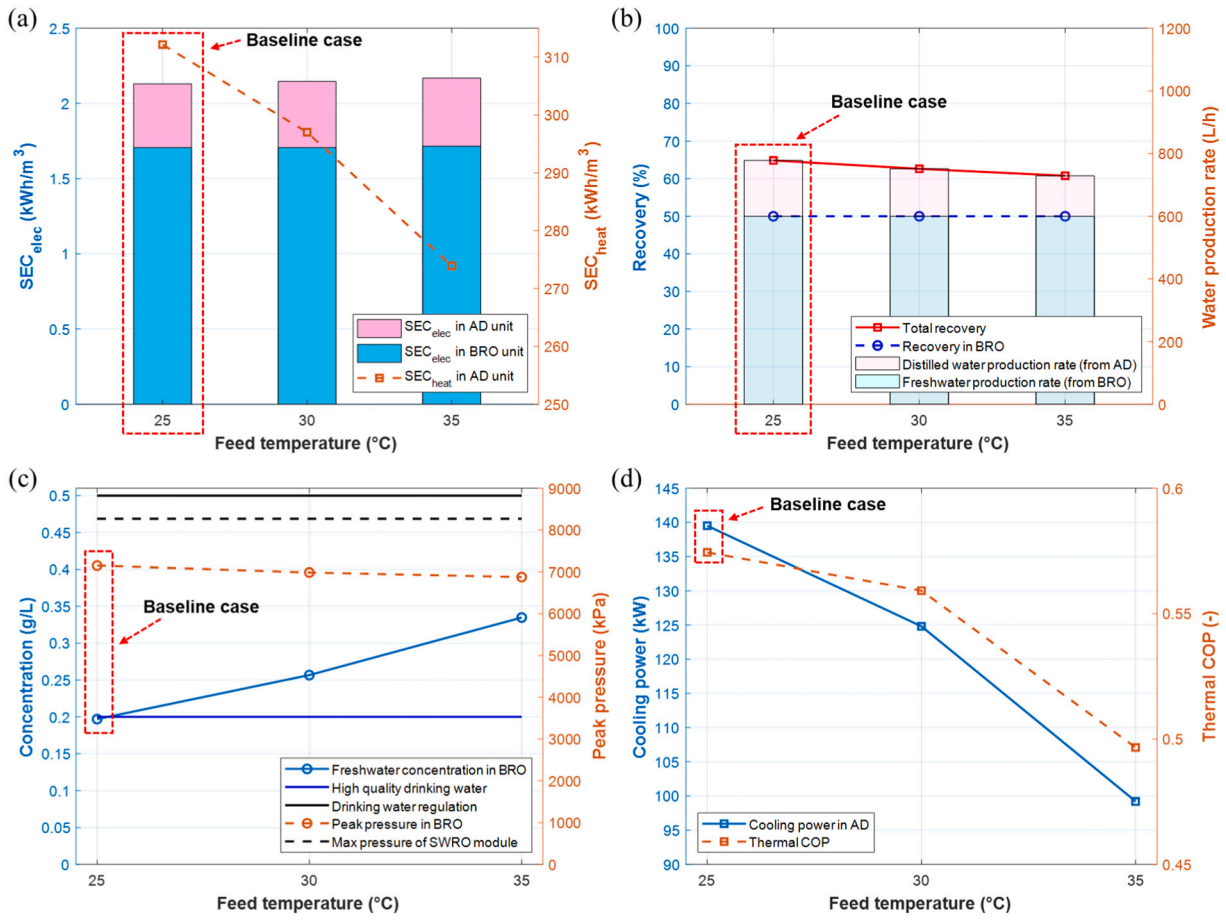

Fig. 7. Effects of feed temperature on the performances of BRO-AD hybrid system for seawater desalination. RO membrane: LG-SW440R (high-rejection membrane) from LG Chem. (a) SEC_{elec} and SEC_{heat}, (b) recovery and water production rate in each unit, (c) permeate quality and peak pressure at RO unit, and (d) cooling power and thermal COP.

effect on the overall SEC_{elec} than in brackish water desalination. At 35 °C, the overall SEC_{elec} and SEC_{heat} are 2.17 kWh/m^3 and 273.9 kWh/m^3, respectively. Compared to the results at 25 °C (2.13 kWh/m^3 of SEC_{elec} and 312.2 kWh/m^3 of SEC_{heat}), slightly higher (almost similar) SEC_{elec} and lower SEC_{heat} occur.

When the feed temperature increases from 25 to 35 °C, overall recovery is reduced from 64.88 % to 60.77 %, while permeate water concentration increases from 0.20 g/L to 0.33 g/L, and the cooling power generation decreases from 139.5 W to 99.21 W (see Fig. 7b, c, and d). Although the permeate water quality still meets drinking water regulation, most aspects of performance deteriorate. This kind of temperature change occurs seasonally in seawater [70], implying that seawater temperature variation should be taken into consideration in the operation of the BRO-AD hybrid system.

3.3. Comparative analysis of BRO, AD, and BRO-AD hybrid systems

The characteristics and advantages of the BRO-AD hybrid system were investigated in the previous sections. However, a comparative analysis of the three systems (BRO alone, AD alone, and BRO-AD hybrid process) is needed to reveal the competitiveness of the BRO-AD hybrid system more clearly. In this section, we analyse brackish and seawater desalination using the same feed concentration as in the baseline cases (3 g/L for brackish water desalination and 35 g/L for seawater desalination). For fair comparison, the recovery is fixed at the baseline cases (95.9 % for brackish water desalination and 64.8 % for seawater desalination) in all systems. Only high-rejection membranes are considered in this section.

3.3.1. Brackish water feed

In brackish water desalination, the SEC_{elec} and SEC_{heat} of AD alone are higher than that of the hybrid system (Fig. 8a). This results from the lower heat transfer coefficient in the evaporator of the AD system, as needed to produce the same water recovery as the hybrid system (95.9 %). The lower heat transfer coefficient is caused by the increase in brine salinity in the flooded evaporator, resulting from higher water recovery, which increases the saturation temperature. While the BRO system does not require any thermal energy, SEC_{elec} of BRO (0.637 kWh/m^3) is slightly higher than that of the hybrid system (0.625 kWh/m^3). When considering SEC_{heat} in the hybrid system (182.4 kWh/m^3), the energy feasibility of BRO alone appears superior. However, as shown in Fig. 8c, a crucial aspect of BRO is that, to reach the same recovery as the hybrid system, the applied pressure would need to be 71.3 bar, which is much higher than the maximum working pressure in a spiral-wound type BWRO membrane module (41 bar). In other words, the BRO operation at the high recovery is impractical using standard membranes. It might become feasible if the membrane were changed to a SWRO type. However, this would increase SEC_{elec} because of lowered permeability [61,64]. In addition, the economic feasibility may be worsened by the increased capital cost of the SWRO membranes and the auxiliary units suitable for such high pressure [61,71,72]. Therefore, the hybrid system is competitive compared to the non-hybrid AD and BRO systems for very high-recovery brackish water desalination in terms of energy economy and practical feasibility.

Comparing the three systems with respect to quality of water output, AD produces pure distilled water, thus having the highest quality. BRO produces the lowest quality because of salt passage through the

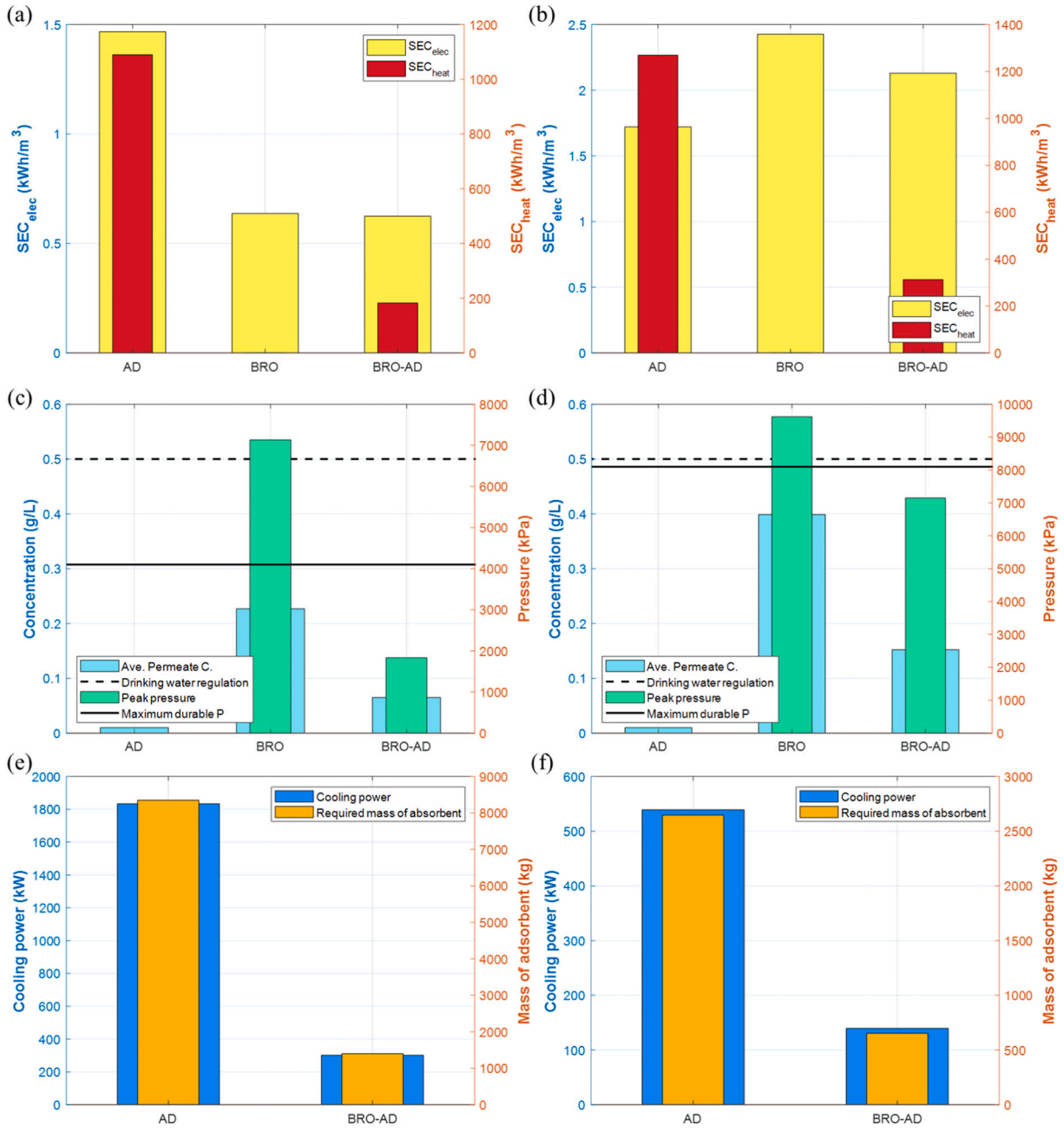

Fig. 8. Comparative analysis results for AD alone, BRO alone, and BRO-AD hybrid. Two cases (3 g/L and 35 g/L) are selected as representative cases for brackish water and seawater desalination, respectively. (a) SEC_{elec} and SEC_{heat} for brackish water desalination, (b) SEC_{elec} and SEC_{heat} for seawater desalination, (c) permeate water quality and peak pressure at RO system for brackish water desalination, (d) permeate water quality and peak pressure at RO system for seawater desalination, (e) cooling power and required mass of absorbent for brackish water desalination, and (f) cooling power and required mass of absorbent for seawater desalination.

membrane (Fig. 8c). The hybrid system produces both high- and low-quality water giving an intermediate quality if blended.

The AD has the highest cooling output at 1834 kW – six times that of the hybrid system (Fig. 8e). However, it also requires six times as much adsorbent (8348 kg instead of 1400 kg), making it an expensive option unless the primary purpose of the system is to provide cooling.

3.3.2. *Seawater feed*

Comparing energy consumption in seawater desalination among the three options, SEC_{elec} of AD is the lowest (1.721 kWh/m^3), while SEC_{heat} is the highest (1270 kWh/m^3) as shown in Fig. 8b. In the hybrid system, 2.130 kWh/m^3 and 312.2 kWh/m^3 are required for SEC_{elec} and SEC_{heat}, respectively. Although BRO requires only SEC_{elec} (2.427 kWh/m^3), the applied pressure (96.22 bar) is much higher than the maximum pressure limitation of the SWRO membrane (82.7 bar) as shown in Fig. 8d. Though AD has many advantages, such as the highest permeate water quality and the largest cooling power among the three options (see Fig. 8d and f) the successful implementation of AD alone as a large-scale seawater desalination system is questionable due to high capital cost and low adsorption rate. Considering all these limitations, the hybrid system is more attractive for high-recovery seawater desalination.

3.3.3. *Effect of feed concentration*

To confirm the competitiveness of the hybrid system, variable feed concentrations from 1.5 to 8 g/L (brackish water desalination) and from 30 to 44 g/L (seawater desalination) were investigated. The same overall

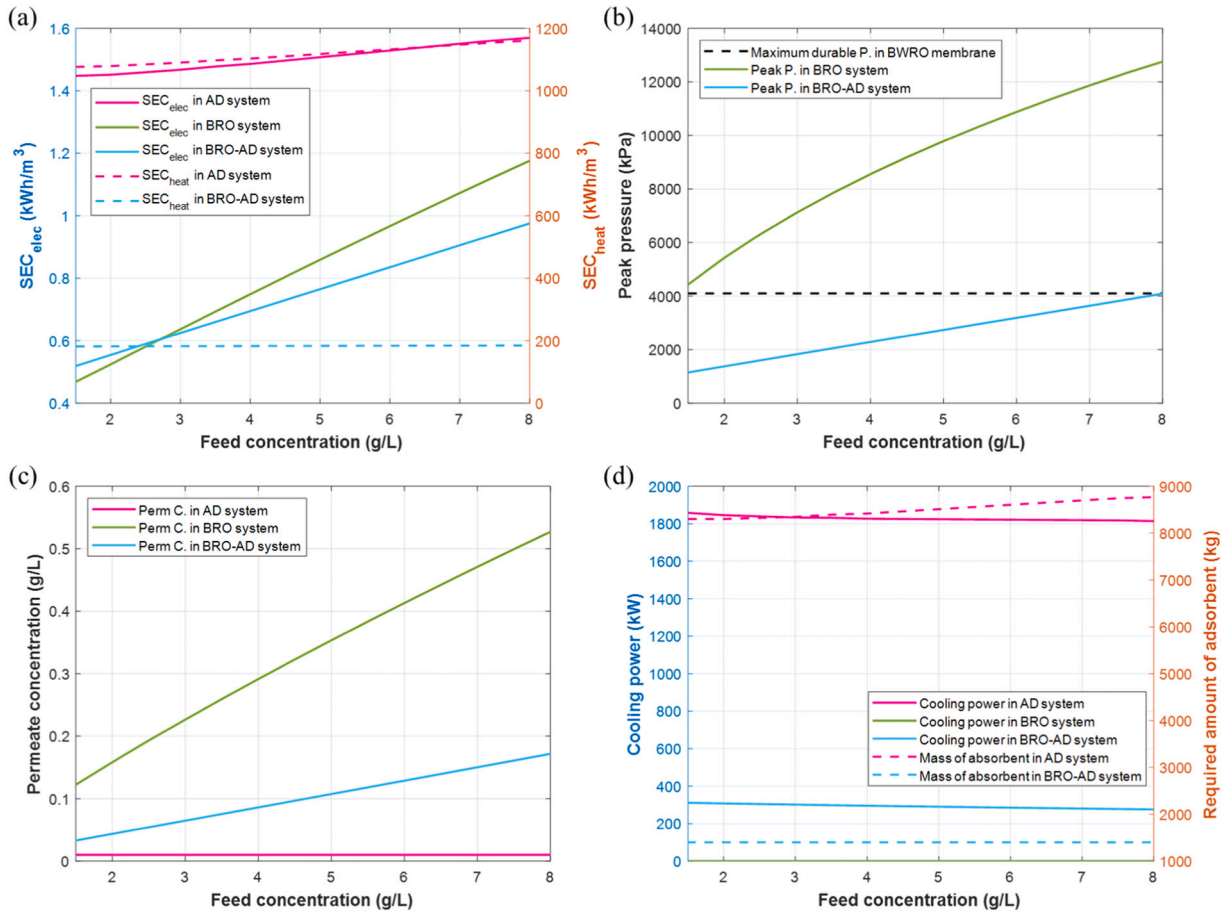

Fig. 9. Comparative analysis results for AD alone, BRO alone, and BRO-AD hybrid depending on feed concentration at brackish water desalination. (a) SEC_{elec} (solid line) and SEC_{heat} (dotted line), (b) peak pressure in RO system (maximum durable pressure of BWRO membrane is denoted as dotted black line), (c) permeate water quality, and (d) cooling power (solid line) and required mass of absorbent (dotted line).

recovery is applied in these systems (BRO alone, AD alone, and the hybrid BRO-AD) for fair comparison. In brackish water desalination, the hybrid system shows the lowest SEC_{elec} compared to either BRO or AD alone, when the feed concentration of brackish water exceeds 2 g/L (Fig. 9a). The energy advantage of the hybrid system over BRO increases with feed concentration. Compared to just AD, the hybrid system has lower SEC_{elec} and SEC_{heat} over the whole range of brackish water feed concentration. As discussed in the previous paragraphs, the BRO may require excessive pressure at high recovery, and this remains true for all the concentrations investigated (Fig. 9b). In contrast, the hybrid system can desalinate the brackish water feed from 1.5 to 8 g/L without any pressure limitation.

As the feed concentration increases, more salt permeates the RO membrane. Fig. 9c shows that the BRO system cannot meet the concentration of the drinking water regulation when the feed concentration of brackish water is higher than 7 g/L. The effects of concentration on the cooling power generation and the required mass of absorbent are not significant (Fig. 9d). Though AD alone provides the largest cooling power, it also demands a large amount of adsorbent material to match the high recovery of the hybrid option. In summary, the hybrid option is an energy-efficient, practical, and multipurpose brackish water desalination system especially at high recovery.

Similar conclusions were obtained for seawater desalination as shown in Fig. 10, which indicates a similar trend as Fig. 8 for all seawater feed concentrations from 30 to 44 g/L. The energy effectiveness in these systems is comparable when considering SEC_{elec} and SEC_{heat} for all feed concentrations (see Fig. 10a). However, as shown in Fig. 10b, BRO cannot operate over 30 g/L feed concentration at this recovery (66 %) given the current pressure limitation; whereas the hybrid system can operate at feed concentration up to 40 g/L. Note that the very high peak pressure in BRO alone is mainly caused by its high recovery (66 %). The permeate water quality of the hybrid system is better than 0.2 g/L over the range of feed concentration (Fig. 10c), making it more applicable to high feed concentration than BRO alone. The permeate water quality in seawater desalination is comparable to that in brackish water desalination, as shown in Figs. 9c and 10c. Because the recovery and the membrane salt permeability with brackish water are much higher than with seawater, a similar permeate water quality can be obtained. AD alone could be considered for high recovery seawater desalination with 30–44 g/L feed concentration, if the large SEC_{heat} and adsorbent mass were not serious drawbacks. Thus, the hybrid system represents an effective solution to increase the water recovery in the seawater application with a feed concentration up to 40 g/L.

3.4. Implementation for ZLD or MLD system

As discussed in Section 3.3, the BRO-AD hybrid system is feasible for a range of brackish and seawater desalination applications up to a feed concentration of 44 g/L. Its advantages of high recovery, applicability for high feed concentration, and multipurpose desalination make it especially interesting given the current research trend in desalination towards ZLD or MLD systems [5,27,67,73].

Even though BRO is an energy-efficient desalination technology at high recovery [14–16,24], there are limitations of maximum working pressure and permeate water quality at the very high recovery (over

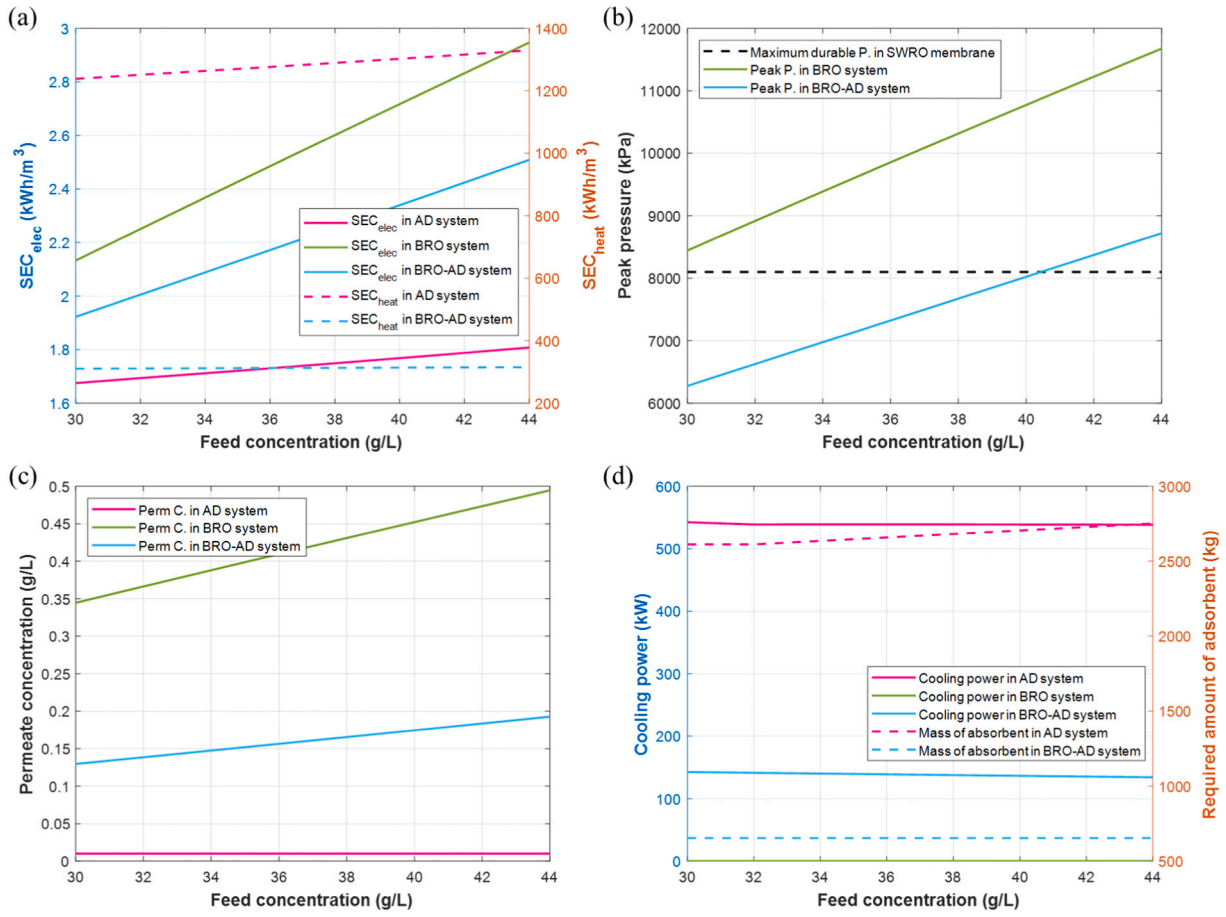

Fig. 10. Comparative analysis results for AD alone, BRO alone, and BRO-AD hybrid depending on feed concentration at seawater desalination. (a) SEC_{elec} (solid line) and SEC_{heat} (dotted line), (b) peak pressure in RO system (maximum durable pressure of SWRO membrane is denoted as dotted black line), (c) permeate water quality, and (d) cooling power (solid line) and required mass of absorbent (dotted line).

95 %) in brackish water desalination. Recently, various processes for brine concentrators using membranes such as high-pressure RO, osmotically assisted RO, and low-salt-rejection RO have been suggested to improve the energy-efficiency. However, current specifications of membranes have restricted the realization of membrane concentrators [74,75]. A BRO-AD hybrid system can achieve high recovery without exceeding membrane pressure limits. AD alone incurs large SEC_{elec} and SEC_{heat} and requires a huge mass of adsorbent materials to reach similar recovery. On the other hand, the energy consumption and operation of AD are not significantly affected by the feed concentration. The BRO-AD hybrid system combines these advantages to provide high-recovery desalination. As a first stage of treatment, BRO system is used because it is effective and efficient up to a certain recovery limit. However, BRO cannot increase the recovery beyond this limit, due to the high osmotic pressure of the brine, such that AD then becomes valuable (provided the fouling or scaling issues are not limiting).

Fouling and scaling issues may arise depending on the precise composition of the feedwater and pre-treatment applied [76]. Seawater contains calcium sulfate which is a sparingly soluble salt that tends to precipitate on the heat transfer surfaces of thermal distillation units. The solubility of calcium sulfate decreases with temperature [77]. Fortunately, the low temperature operation of the AD unit (<35 °C) favours high solubility and decreases the tendency for calcium sulfate precipitation in the proposed system. For brackish water, the composition depends heavily on location. Calcium salts such as calcium carbonate are common causes of fouling, as are colloidal silica, clay, and iron oxide. The desalination industry has developed a number of pre-treatment and anti-scaling technologies to reduce and manage the risk of fouling even at high recoveries.

The advantage of the BRO-AD hybrid is therefore appropriate for ZLD and MLD systems while working within the pressure limitations of most membranes [67]. Currently, ZLD or MLD typically relies on energy-intensive thermal-based systems [5,67,78]. The results in this study revealed the potential of the BRO-AD hybrid system for energy-efficient MLD. However, various issues such as fouling/scaling alleviation at high recovery need to be resolved prior to implementation. In addition, cost calculations and life-cycle analyses should be carried out to investigate the actual applicability of the BRO-AD hybrid system. Because the current technological readiness level of the BRO-AD hybrid system is still at the pilot stage (TRL5), the economic analysis needs to be carried out once further development has taken place. Through the current study, the advantages of the BRO-AD hybrid system in terms of energy, recovery, and versatility have been highlighted. Future work should include an economic feasibility study.

4. Conclusions

This study has investigated comprehensively the feasibility of hybrid batch reverse osmosis (BRO)-adsorption desalination (AD) in terms of specific energy consumption, recovery, cooling power generation, and suitability for brackish and seawater desalination. The results show high potential for minimal/zero liquid discharge with modest energy consumption even at high recovery – above the recovery practical using non-hybrid BRO or AD. The key findings are:

1. To connect the BRO unit and AD unit for continuous operation, multiple BRO units should be connected in parallel and operated sequentially to provide a continuous brine flow to the AD and eliminate the need for an intermediate buffer tank.
2. Very high recoveries of 94.1–96.9 % (brackish water) and 64.0–65.3 % (seawater) are obtained in the BRO-AD hybrid with feed concentrations of 1–8 g/L and 30–44 g/L, respectively (at 25 °C). The specific energy consumptions are in the range of 0.395–0.884 kWh/m^3 (SEC_{elec}) and 181.2–184.4 kWh/m^3 (SEC_{heat}) for brackish water desalination, and 1.923–2.509 kWh/m^3 (SEC_{elec}) and 310.4–315.1 kWh/m^3 (SEC_{heat}) for seawater desalination. Two water qualities (distilled water and potable water) can be produced simultaneously. Additionally, cooling production (277.7–315.7 kW from brackish water desalination and 168.5–183.6 kW from seawater desalination) is also provided by the evaporator of the AD system, beside the distilled water production.
3. The hybrid system withstands severe conditions such as high concentration and high temperature feed solution. It can handle a range of feed concentration (1–8 g/L for brackish water and 30–44 g/L for seawater) and temperature (25–35 °C) without any change in process configuration or membrane type. Given the current rising demand for hypersaline water desalination, it offers a competitive solution for the treatment of hypersaline water with low energy and high recovery, while providing multipurpose desalination.
4. The hybrid system has better performances in terms of permeate quality and energy consumption than non-hybrid BRO or AD. The pressure limit of the membrane, and the large mass of absorbent required, are the main barriers preventing high recovery using BRO and AD respectively. The recovery in the BRO-AD hybrid is not limited by the membrane, enabling recoveries of >90 % to be readily achieved using brackish water and >60 % using seawater. Thus, BRO-AD has the highest potential for minimal/zero liquid discharge system.

CRediT authorship contribution statement

KP: Writing - Original Draft, analysis and modelling.
IA: Writing - Original Draft, analysis and modelling.
PD: Conceptualization, theory, writing – review & editing, supervision, funding acquisition.
RA: Conceptualisation, writing, supervision – review & editing.
SM: Conceptualisation, writing – review & editing.
MI: Review & editing, background investigation.
MA: Review & editing, background investigation.

Declaration of competing interest

The authors declare that they have no known competing financial interests or personal relationships that could have appeared to influence the work reported in this paper.

Acknowledgements

The authors extend their appreciation to the Deputyship for Research & Innovation, Ministry of Education in Saudi Arabia for funding this research work through the project number 969.

References

[1] M. Elimelech, W.A. Phillip, The future of seawater desalination: energy, technology, and the environment, Science 333 (2011) 712–717.
[2] J. Kim, K. Park, D.R. Yang, S. Hong, A comprehensive review of energy consumption of seawater reverse osmosis desalination plants, Appl. Energy 254 (2019), 113652.
[3] K. Park, J. Kim, D.R. Yang, S. Hong, Towards a low-energy seawater reverse osmosis desalination plant: a review and theoretical analysis for future directions, J. Membr. Sci. 595 (2020), 117607.
[4] J. Eke, A. Yusuf, A. Giwa, A. Sodiq, The global status of desalination: an assessment of current desalination technologies, plants and capacity, Desalination 495 (2020), 114633.
[5] C. Boo, I.H. Billinge, X. Chen, K.M. Shah, N.Y. Yip, Zero liquid discharge of ultrahigh-salinity brines with temperature swing solvent extraction, Environ. Sci. Technol. 54 (2020) 9124–9131.
[6] E. Jones, M. Qadir, M.T. van Vliet, V. Smakhtin, S.-M. Kang, The state of desalination and brine production: a global outlook, Sci. Total Environ. 657 (2019) 1343–1356.
[7] J.-H. Bang, S.-C. Chae, K. Song, S.-W. Lee, Optimizing experimental parameters in sequential CO2 mineralization using seawater desalination brine, Desalination 519 (2021), 115309.
[8] M.W. Shahzad, M. Burhan, L. Ang, K.C. Ng, Energy-water-environment nexus underpinning future desalination sustainability, Desalination 413 (2017) 52–64.
[9] A. Subramani, M. Badruzzaman, J. Oppenheimer, J.G. Jacangelo, Energy minimization strategies and renewable energy utilization for desalination: a review, Water Res. 45 (2011) 1907–1920.
[10] J.L. Prante, J.A. Ruskowitz, A.E. Childress, A. Achilli, RO-PRO desalination: an integrated low-energy approach to seawater desalination, Appl. Energy 120 (2014) 104–114.
[11] T.H. Chong, S.-L. Loo, W.B. Krantz, Energy-efficient reverse osmosis desalination process, J. Membr. Sci. 473 (2015) 177–188.
[12] H. Wang, Low-energy desalination, Nat. Nanotechnol. 13 (2018) 273–274.
[13] F. Chen, J. Wang, C. Feng, J. Ma, T.D. Waite, Low energy consumption and mechanism study of redox flow desalination, Chem. Eng. J. 401 (2020), 126111.
[14] K. Park, P.A. Davies, A compact hybrid batch/semi-batch reverse osmosis (HBSRO) system for high-recovery, low-energy desalination, Desalination 504 (2021), 114976.
[15] K. Park, L. Burlace, N. Dhakal, A. Mudgal, N.A. Stewart, P.A. Davies, Design, modelling and optimisation of a batch reverse osmosis (RO) desalination system using a free piston for brackish water treatment, Desalination 494 (2020), 114625.
[16] J.R. Werber, A. Deshmukh, M. Elimelech, Can batch or semi-batch processes save energy in reverse-osmosis desalination? Desalination 402 (2017) 109–122.
[17] S. Cordoba, A. Das, J. Leon, J.M. Garcia, D.M. Warsinger, Double-acting batch reverse osmosis configuration for best-in-class efficiency and low downtime, Desalination 506 (2021), 114959.
[18] M. Li, Dynamic operation of batch reverse osmosis and batch pressure retarded osmosis, Ind. Eng. Chem. Res. 59 (2020) 3097–3108.
[19] S. Lin, M. Elimelech, Staged reverse osmosis operation: configurations, energy efficiency, and application potential, Desalination 366 (2015) 9–14.
[20] S. Lin, S. Veerapaneni, Emerging investigator series: toward the ultimate limit of seawater desalination with mesopelagic open reverse osmosis, Environ. Sci.: Water Res. Technol. 7 (2021) 1212–1219, https://doi.org/10.1039/D1EW00153A.
[21] P.A. Davies, J. Wayman, C. Alatta, K. Nguyen, J. Orfi, A desalination system with efficiency approaching the theoretical limits, Desalin. Water Treat. 57 (2016) 23206–23216.
[22] H. Abu Ali, M. Baronian, L. Burlace, P.A. Davies, S. Halasah, M. Hind, A. Hossain, C. Lipchin, A. Majali, M. Mark, Off-grid desalination for irrigation in the Jordan Valley, Desalin.Water Treat. 168 (2019) 143–154.
[23] E. Hosseinipour, K. Park, L. Burlace, T. Naughton, P.A. Davies, A free-piston batch reverse osmosis (RO) system for brackish water desalination: experimental study and model validation, Desalination 527 (2022), 115524.
[24] Q.J. Wei, C.I. Tucker, P.J. Wu, A.M. Trueworthy, E.W. Tow, Impact of salt retention on true batch reverse osmosis energy consumption: experiments and model validation, Desalination 479 (2020), 114177.
[25] L. Burlace, P. Davies, Fouling and fouling mitigation in batch reverse osmosis: review and outlook, Desalin. Water Treat. 249 (2022) 1–22.
[26] J. Swaminathan, E.W. Tow, R.L. Stover, Practical aspects of batch RO design for energy-efficient seawater desalination, Desalination 470 (2019), 114097.
[27] Z. Wang, A. Deshmukh, Y. Du, M. Elimelech, Minimal and zero liquid discharge with reverse osmosis using low-salt-rejection membranes, Water Res. 170 (2020), 115317.
[28] D.M. Davenport, L. Wang, E. Shalusky, M. Elimelech, Design principles and challenges of bench-scale high-pressure reverse osmosis up to 150 bar, Desalination 517 (2021), 115237.
[29] K.C. Ng, K. Thu, Y. Kim, A. Chakraborty, G. Amy, Adsorption desalination: an emerging low-cost thermal desalination method, Desalination 308 (2013) 161–179.
[30] A.S. Alsaman, A.A. Askalany, K. Harby, M.S. Ahmed, A state of the art of hybrid adsorption desalination–cooling systems, Renew. Sust. Energ. Rev. 58 (2016) 692–703.
[31] M.S. Atab, A. Smallbone, A. Roskilly, A hybrid reverse osmosis/adsorption desalination plant for irrigation and drinking water, Desalination 444 (2018) 44–52.
[32] E.S. Ali, A.S. Alsaman, K. Harby, A.A. Askalany, M.R. Diab, S.M.E. Yakoot, Recycling brine water of reverse osmosis desalination employing adsorption desalination: a theoretical simulation, Desalination 408 (2017) 13–24.
[33] H. Ma, J. Zhang, C. Liu, X. Lin, Y. Sun, Experimental investigation on an adsorption desalination system with heat and mass recovery between adsorber and desorber beds, Desalination 446 (2018) 42–50.
[34] I. Albaik, M.B. Elsheniti, R. Al-Dadah, S. Mahmoud, İ. Solmaz, Numerical and experimental investigation of multiple heat exchanger modules in cooling and desalination adsorption system using metal organic framework, Energy Convers. Manag. 251 (2022), 114934.

[35] E. Elsayed, A.-D. Raya, S. Mahmoud, P. Anderson, A. Elsayed, Experimental testing of aluminium fumarate MOF for adsorption desalination, Desalination 475 (2020), 114170.
[36] P.G. Youssef, H. Dakkama, S.M. Mahmoud, R.K. AL-Dadah, Experimental investigation of adsorption water desalination/cooling system using CPO-27Ni MOF, Desalination 404 (2017) 192–199.
[37] M.W. Shahzad, K.C. Ng, K. Thu, B.B. Saha, W.G. Chun, Multi effect desalination and adsorption desalination (MEDAD): a hybrid desalination method, Appl. Therm. Eng. 72 (2014) 289–297.
[38] E.S. Ali, R.H. Mohammed, N.A. Qasem, S.M. Zubair, A. Askalany, Solar-powered ejector-based adsorption desalination system integrated with a humidification-dehumidification system, Energy Convers. Manag. 238 (2021), 114113.
[39] K. Harby, E.S. Ali, K. Almohammadi, A novel combined reverse osmosis and hybrid absorption desalination-cooling system to increase overall water recovery and energy efficiency, J. Clean. Prod. 287 (2021), 125014.
[40] I.I. El-Sharkawy, K. Uddin, T. Miyazaki, B.B. Saha, S. Koyama, H.-S. Kil, S.-H. Yoon, J. Miyawaki, Adsorption of ethanol onto phenol resin based adsorbents for developing next generation cooling systems, Int. J. Heat Mass Transf. 81 (2015) 171–178.
[41] H.W.B. Teo, A. Chakraborty, B. Han, Water adsorption on CHA and AFI types zeolites: modelling and investigation of adsorption chiller under static and dynamic conditions, Appl. Therm. Eng. 127 (2017) 35–45.
[42] E. Elsayed, A.-D. Raya, S. Mahmoud, A. Elsayed, P.A. Anderson, Aluminium fumarate and CPO-27 (Ni) MOFs: characterization and thermodynamic analysis for adsorption heat pump applications, Appl. Therm. Eng. 99 (2016) 802–812.
[43] T. Qiu, P. Davies, Concentration polarization model of spiral-wound membrane modules with application to batch-mode RO desalination of brackish water, Desalination 368 (2015) 36–47.
[44] D.M. Warsinger, E.W. Tow, K.G. Nayar, L.A. Maswadeh, Energy efficiency of batch and semi-batch (CCRO) reverse osmosis desalination, Water Res. 106 (2016) 272–282.
[45] J. Kim, S. Hong, A novel single-pass reverse osmosis configuration for high-purity water production and low energy consumption in seawater desalination, Desalination 429 (2018) 142–154.
[46] C.P. Koutsou, S.G. Yiantsios, A.J. Karabelas, A numerical and experimental study of mass transfer in spacer-filled channels: effects of spacer geometrical characteristics and Schmidt number, J. Membr. Sci. 326 (2009) 234–251.
[47] R. Darby, R.P. Chhabra, Chemical Engineering Fluid Mechanics, CRC Press, 2016.
[48] J. Kim, K. Park, S. Hong, Application of two-stage reverse osmosis system for desalination of high-salinity and high-temperature seawater with improved stability and performance, Desalination 492 (2020), 114645.
[49] E. Glueckauf, Theory of chromatography. Part 10.—Formulæ for diffusion into spheres and their application to chromatography, Trans. Faraday Society 51 (1955) 1540–1551.
[50] I. Albaik, R. Al-Dadah, S. Mahmoud, M.K. Almesfer, M.A. Ismail, E. Elsayed, M. Saleh, A comparison between the packed and coated finned tube for adsorption system using aluminium fumarate: numerical study, Therm. Sci. Eng. Progress 22 (2021), 100859.
[51] A.R.M. Rezk, Theoretical and Experimental Investigation of Silica Gel/Water Adsorption Refrigeration Systems, University of Birmingham, 2012.
[52] Y.A. Çengel, J.M. Cimbala, Fluid Mechanics: Fundamentals and Applications, McGraw-Hill Higher Education, 2010.
[53] A. Ruiz-García, E. Ruiz-Saavedra, 80,000 h operational experience and performance analysis of a brackish water reverse osmosis desalination plant. Assessment of membrane replacement cost, Desalination 375 (2015) 81–88.
[54] N. Voutchkov, Energy use for membrane seawater desalination–current status and trends, Desalination 431 (2018) 2–14.
[55] B.A. Qureshi, S.M. Zubair, Exergetic analysis of a brackish water reverse osmosis desalination unit with various energy recovery systems, Energy 93 (2015) 256–265.
[56] A. Hasan, B. Mugdadi, B. Tashtoush, A.-N. Moh'd A, Direct and indirect utilization of thermal energy for cooling generation: a comparative analysis, Energy 238 (2022) 122046.
[57] E. Galloni, G. Fontana, S. Staccone, Design and experimental analysis of a mini ORC (organic rankine cycle) power plant based on R245fa working fluid, Energy 90 (2015) 768–775.
[58] M.S. Lee, J.W. Chang, K. Park, D.R. Yang, Energetic and exergetic analyses of a closed-loop pressure retarded membrane distillation (PRMD) for low-grade thermal energy utilization and freshwater production, Desalination 534 (2022), 115799.
[59] W. Jantaporn, A. Ali, P. Aimar, Specific energy requirement of direct contact membrane distillation, Chem. Eng. Res. Des. 128 (2017) 15–26.
[60] R. Singh, Analysis of high recovery brackish water desalination processes using fuel cells, Sep. Sci. Technol. 44 (2009) 585–598.
[61] K.M. Sassi, I.M. Mujtaba, MINLP based superstructure optimization for boron removal during desalination by reverse osmosis, J. Membr. Sci. 440 (2013) 29–39.
[62] Y.-Y. Lu, Y.-D. Hu, X.-L. Zhang, L.-Y. Wu, Q.-Z. Liu, Optimum design of reverse osmosis system under different feed concentration and product specification, J. Membr. Sci. 287 (2007) 219–229.
[63] X. Chen, N.Y. Yip, Unlocking high-salinity desalination with cascading osmotically mediated reverse osmosis: energy and operating pressure analysis, Environ. Sci. Technol. 52 (2018) 2242–2250.
[64] J. Kim, K. Park, S. Hong, Optimization of two-stage seawater reverse osmosis membrane processes with practical design aspects for improving energy efficiency, J. Membr. Sci. 601 (2020), 117889.
[65] X. Chen, C. Boo, N.Y. Yip, Transport and structural properties of osmotic membranes in high-salinity desalination using cascading osmotically mediated reverse osmosis, Desalination 479 (2020), 114335.
[66] A. Das, D.M. Warsinger, Batch counterflow reverse osmosis, Desalination 507 (2021), 115008.
[67] A.A. Atia, N.Y. Yip, V. Fthenakis, Pathways for minimal and zero liquid discharge with enhanced reverse osmosis technologies: module-scale modeling and techno-economic assessment, Desalination 509 (2021), 115069.
[68] W.H. Bruvold, H.J. Ongerth, Taste quality of mineralized water, Journal-American Water Works Association 61 (1969) 170–174.
[69] C. Koutsou, E. Kritikos, A. Karabelas, M. Kostoglou, Analysis of temperature effects on the specific energy consumption in reverse osmosis desalination processes, Desalination 476 (2020), 114213.
[70] C. Periyasamy, P. Anantharaman, T. Balasubramanian, P.S. Rao, Seasonal variation in growth and carrageenan yield in cultivated Kappaphycus alvarezii (Doty) Doty on the coastal waters of Ramanathapuram district, Tamil Nadu, J. Appl. Phycol. 26 (2014) 803–810.
[71] A. Malek, M. Hawlader, J. Ho, Design and economics of RO seawater desalination, Desalination 105 (1996) 245–261.
[72] K. Park, D.Y. Kim, D.R. Yang, Cost-based feasibility study and sensitivity analysis of a new draw solution assisted reverse osmosis (DSARO) process for seawater desalination, Desalination 422 (2017) 182–193.
[73] A. Panagopoulos, Energetic, economic and environmental assessment of zero liquid discharge (ZLD) brackish water and seawater desalination systems, Energy Convers. Manag. 235 (2021), 113957.
[74] A. Giwa, V. Dufour, F.Al Marzooqi, M.Al Kaabi, S. Hasan, Brine management methods: recent innovations and current status, Desalination 407 (2017) 1–23.
[75] K. Park, J. Kim, S. Hong, Brine management systems using membrane concentrators: future directions for membrane development in desalination, Desalination 535 (2022), 115839.
[76] P. Goh, W. Lau, M. Othman, A. Ismail, Membrane fouling in desalination and its mitigation strategies, Desalination 425 (2018) 130–155.
[77] E.P. Partridge, A.H. White, The solubility of calcium sulfate from 0 to 200, J. Am. Chem. Soc. 51 (1929) 360–370.
[78] T. Tong, M. Elimelech, The global rise of zero liquid discharge for wastewater management: drivers, technologies, and future directions, Environ. Sci. Technol. 50 (2016) 6846–6855.